NASA Technical Paper 1446

Investigation of Effects of Background Water on Upwelled Reflectance Spectra and Techniques for Analysis of Dilute Primary-Treated Sewage Sludge

Charles H. Whitlock, J. W. Usry, William G. Witte,
Franklin H. Farmer, and E. A. Gurganus

AUGUST 1979

NASA

NASA Technical Paper 1446

Investigation of Effects of Background Water on Upwelled Reflectance Spectra and Techniques for Analysis of Dilute Primary-Treated Sewage Sludge

Charles H. Whitlock, J. W. Usry, William G. Witte,
Franklin H. Farmer, and E. A. Gurganus
Langley Research Center
Hampton, Virginia

NASA

SUMMARY

In an effort to improve understanding of the effects of variations in background water on reflectance spectra, laboratory tests have been conducted with various concentrations of sewage sludge diluted with several types of background water. The results from these tests indicate that reflectance spectra for sewage-sludge mixtures are dependent upon the reflectance of the background water. Both the ratio of sewage-sludge reflectance to background-water reflectance and the ratio of the difference in reflectance to background-water reflectance show spectral variation for different turbid background waters. The difference in reflectance is the only parameter considered in this study which does not have major spectral variations with different background waters.

INTRODUCTION

The National Aeronautics and Space Administration (NASA), in cooperation with the Environmental Protection Agency (EPA) and the National Oceanic and Atmospheric Administration (NOAA), is conducting a research program to evaluate the feasibility of remotely monitoring ocean dumping of waste products such as industrial wastes and sewage sludge. The program consists of both field experiments (refs. 1 to 8) and laboratory studies (refs. 8 to 10). As a result of the expense involved, the field results have generally been limited to one experiment with a specific discharge. Repeat experiments to investigate the reliability of data-analysis algorithms and the effects of variations in background water and atmospheric interference have not been conducted. In an effort to improve this situation, a series of laboratory tests has been conducted to investigate the effects of variations in background water on a single pollutant, dilute primary-treated sewage sludge from the Southwest Philadelphia Waste Treatment Facility. It is the purpose of this paper to describe how upwelled reflectance spectra of dilute sewage-sludge mixtures changed as the content of chlorophyll a and suspended solids in the background water varied. In addition, several types of data-analysis algorithms are applied to the laboratory data to investigate the sensitivity of each algorithm to variations in background water. It is expected that such information from laboratory tests will aid in the selection of algorithms to be used in future field experiments.

Use of trade names or names of manufacturers in this report does not constitute an official endorsement of such products or manufacturers, either expressed or implied, by the National Aeronautics and Space Administration.

SYMBOLS

A   area of spectrometer entrance slit, cm^2

B $[\rho_u(\lambda)]_{bw} L_{so}(\lambda) = [L_u(\lambda)]_{bw}$, $mW/cm^2\text{-}sr\text{-}nm$

C	$L_{rd}(\lambda) + L_{rs}(\lambda) + L_a(\lambda)/T_a(\lambda)$, mW/cm^2-sr-nm
D	vertical displacement of oscilloscope measurement, cm
$E(\lambda)$	spectral irradiance, W/m^2-nm
K	ratio of instrument throughput to vertical-scale sensitivity factor, $\dfrac{cm^2\text{-sr}}{mW/nm\text{-cm}}$
$L_a(\lambda)$	upwelled radiance from light scattered into receiver by the atmosphere, mW/cm^2-sr-nm
$L_{rd}(\lambda)$	upwelled radiance from specular reflection of diffuse skylight, mW/cm^2-sr-nm
$L_{rs}(\lambda)$	upwelled radiance from specular reflection of sunlight, mW/cm^2-sr-nm
$L_{so}(\lambda)$	upwelled radiance above water surface from 100-percent diffuse reflector, mW/cm^2-sr-nm
$L_u(\lambda)$	inherent upwelled spectral radiance above water surface, mW/cm^2-sr-nm
$L_z(\lambda)$	apparent upwelled spectral radiance at altitude z, mW/cm^2-sr-nm
$\Delta[L_z(\lambda)]_{ss}$	$= [L_z(\lambda)]_{ss} - [L_z(\lambda)]_{bw}$, mW/cm^2-sr-nm
$P(\lambda)$	spectral power, mW/nm
S	vertical-scale sensitivity factor, mW/cm-nm
$T_a(\lambda)$	atmospheric transmission fraction
α	beam attenuation coefficient at $\lambda = 510$ nm, m^{-1}
λ	wavelength, nm
$\rho_u(\lambda)$	inherent upwelled spectral reflectance above water surface, percent of input (relative to a 100-percent diffuse reflector)
$\Delta[\rho_u(\lambda)]_{ss}$	$= [\rho_u(\lambda)]_{ss} - [\rho_u(\lambda)]_{bw}$, percent of input
$\Delta[\rho_u(\lambda)]_{ss}^{*}$	$= [\rho_u(\lambda)]_{ss} - [\rho_u(\lambda)]_{ss=4ppm}$, percent of input
σ	standard deviation of measurement error
Ω	acceptance solid angle of spectrometer, sr

Subscripts:

bw   background water

ss   sewage sludge mixed with background water

<div align="center">EXPERIMENTAL METHOD</div>

The arrangement shown in figure 1 was used for the laboratory tests. Major parts of the system include a water tank, circulation system, filtration and deionization system, solar simulator, first-surface mirror, and rapid-scan spectrometer. The light source is a 2.5-kW xenon short-arc lamp which produces a spectrum similar to that of the Sun at a solar elevation angle of 30°, as shown in figure 2. A more complete description of the laboratory and equipment is given in appendix A.

Approximately 4 weeks prior to the laboratory spectral-signature tests, cultures of Phaeodactylon tricornutum (a golden-brown algae) were added to a 2-liter laboratory container of artificial seawater which had been prepared in accordance with reference 11. (See table I.) The nutrients in table II were added and artificial sunlight was used to grow the algae in a laboratory environment. When cell count increased such that chlorophyll a concentration exceeded 500 μg/ℓ, the mixture was transferred to a 95-liter tank which had previously been filled with artificial seawater. Nutrients were added to the diluted algae mixture and growth was continued under artificial sunlight for several weeks. When chlorophyll a concentration was again in excess of 500 μg/ℓ, the mixture was transferred to a 341-liter tank and growth was allowed to continue. The desire was to achieve chlorophyll a concentrations between 700 and 800 μg/ℓ in the 341-liter container. Portions of this mixture would then be added to the 11 600-liter tank shown in figure 1 to achieve mixtures with the desired algae content.

The 11 600-liter tank was then filled with tap water that had been filtered and deionized such that it contained less than 0.5 ppm of total suspended solids and less than 2 ppm of dissolved ionic substances. The chemical compounds in table I were added in sequence in the amounts shown after each preceding compound had been observed to dissolve in the water mixture. The final artificial seawater mixture was then filtered for 15 hours such that concentration of total suspended solids was less than 0.1 ppm and concentration of chlorophyll a was less than 0.2 μg/ℓ.

The sequence of laboratory tests is summarized in figure 3. The high value of total suspended solids shown for artificial seawater plus nutrients (mixture 0) is believed to have been caused by incomplete dissolution of the powdered nutrients in the artificial seawater prior to the addition of algae. A portion of the mixture in the 341-liter tank (chlorophyll a = 740 μg/ℓ, and total suspended solids = 43 ppm) was added to the 11 600-liter tank. The resulting water had a chlorophyll a concentration of 7 μg/ℓ and is labeled mixture 1 in figure 3 and table III. This is the first mixture for which upwelled

3

spectral-reflectance measurements are presented. Two additional water transfers were made later in the day to obtain mixtures 2 and 3, which had chlorophyll a concentrations of 15 and 20 µg/ℓ, respectively. Artificial light was then added and the algae allowed to grow for 17 hours to obtain mixture 4. The next morning, analyses were made of mixture 4, which had a chlorophyll a concentration of 31 µg/ℓ and a total suspended-solids concentration of 11.6 ppm. After measurement of the upwelled reflectance spectra, two additions of primary-treated sewage sludge were made such that total suspended-solids concentration increased from 11.6 ppm in mixture 4 to 19.3 ppm in mixture 5 and 48.7 ppm in mixture 6. Table III indicates that algae cell count remained essentially constant.

Upwelled radiance over the wavelength range from 400 to 980 nm was measured for each of the six water mixtures in table III over the 2-day period of the tests. For each water mixture, diffuse reflectance measurements of the solar-simulator spectral input at the water surface were made with a 99-percent-reflectance white card to monitor optical stability of the laboratory system and to derive spectral reflectance from upwelled radiance values as described in appendix A.

RESULTS AND DISCUSSION

Artificial Seawater Tests

Measured spectral radiance and reflectance curves are shown in figures 4(a) and 4(b), respectively, for mixtures 1 through 4. All data are for a spectral resolution equal to 32 nm. Estimated values for standard deviation σ are based on manufacturer's specifications (see appendix A) combined with data readup inaccuracy. Not included in the estimates of standard deviation are the uncertainties in the concentrations of chlorophyll a and total suspended solids inherent in laboratory analyses of water samples. Standard deviation of chlorophyll a concentrations is estimated at 20 percent of the observed value. (All chlorophyll a values given in this report are the average of three measurements.) Estimated standard deviation of total suspended-solids values is 25 percent at 7 ppm and 10 percent at 50 ppm. Variations in the spectral-radiance curves (fig. 4(a)) are caused in part by the spectral characteristics of the xenon-lamp input source (see fig. 2(b)). Figure 4(b) shows spectral-reflectance values which cancel the effects of the lamp spectra. Figure 4(b) shows little change in reflectance for chlorophyll a concentrations between 7 and 20 µg/ℓ for the Phaeodactylon tricornutum algae species. As higher concentrations of chlorophyll a are approached with mixture 4, a larger increase in spectral reflectance is observed.

Spectral-radiance and reflectance values are shown in figures 5(a) and 5(b), respectively, for mixtures 4, 5, and 6. Mixture 4 is considered to be a turbid background-water mixture to which two quantities of sewage sludge were added to obtain mixtures 5 and 6. In figure 5(b), it appears that the addition of sewage sludge from the Southwest Philadelphia Waste Treatment Facility causes reflectance to increase by a nearly constant amount, within the accuracy of the measurements over the spectral range from 400 to 980 nm.

Comparison With Previous Results

Dilute primary-treated sewage sludge from the Southwest Philadelphia Waste Treatment Facility has previously been tested and the results reported in reference 9. Those tests were conducted with both filtered, deionized tap water and natural water pumped from the Back River at Hampton, Virginia. Figure 6(a) shows reflectance spectra from the reference 9 tests compared with the curve from figure 5(b) for the mixture with a sewage-sludge concentration of 37 ppm (mixture 6). This curve for mixture 6 will be considered as representative of a 34-ppm mixture for the remainder of this publication, since the difference is within repeatability of water sample analysis. Figure 6(a) indicates that reflectance spectra for the two samples of sewage sludge at a concentration of 34 ppm are different. Figure 6(b) shows reflectance spectra for two of the background waters, mixture 4 and Back River water. A reflectance spectrum for filtered, deionized tap water is not shown because of limitations of the laboratory system. (See appendix A.) Comparison of figure 6(a) with figure 6(b) indicates that the spectral-reflectance variation of each sewage-sludge mixture is quite similar to that of the background water for both mixture 4 and Back River water.

Application of Selected Algorithms

As discussed previously, one purpose of this study was to investigate the sensitivity to variations in background water of several algorithms for analysis of field data by use of laboratory reflectance data. In order to accomplish this, it is first necessary to relate upwelled radiance measurements at altitude to surface-reflectance values. An analytical expression for this relation is given in appendix B, along with similar equations for several algorithms. In the following paragraphs, laboratory reflectance values will be applied to these algorithms in an effort to infer probable characteristics of remote-sensing radiance measurements from aircraft or satellites.

The ratio of sewage-sludge to background-water apparent radiance is related to the ratio of sewage-sludge reflectance to background-water inherent reflectance as shown in the following equation (which is equal to eq. (B3)):

$$\frac{[L_z(\lambda)]_{ss}}{[L_z(\lambda)]_{bw}} = \frac{\{[\rho_u(\lambda)]_{ss}/[\rho_u(\lambda)]_{bw}\}B + C}{B + C} \tag{1}$$

Application of laboratory values from figure 6 produces the spectra of inherent-reflectance ratios shown in figure 7. Figure 7(a) shows curves based on continuous spectrometer data. Simulated values for bands 2 through 9 of the Modular Multispectral Scanner (M^2S, Bendix Corp.) instrument have also been calculated and are shown in figure 7(b). These calculations were made by integrating the values of figure 7(a) over the bandwidths of 40 to 100 nm for each channel of the M^2S instrument. The M^2S instrument was chosen for simulation because of its wide use in ocean-dumping remote-sensing experiments (refs. 5 to 7, for example). Figure 7(a) indicates a difference in $[\rho_u(\lambda)]_{ss}/[\rho_u(\lambda)]_{bw}$ for different turbid background waters. The sharp peaks observed in the laboratory

5

spectra are not evident in the simulated M^2S spectra because of the poorer spectral resolution of that instrument. If the spectral characteristics of the ratio of sewage-sludge reflectance to background-water reflectance vary with differences in turbid background water, it is reasonable to expect that the ratio of sewage-sludge radiance to background-water apparent radiance at altitude z will also vary according to equation (1).

Another algorithm which has some potential for identification of marine pollutants is one in which the difference between the sewage-sludge radiance and background-water apparent radiance $\Delta[L_z(\lambda)]_{ss}$ is expressed as a ratio to the apparent radiance of the background water $[L_z(\lambda)]_{bw}$. This ratio is related to inherent-reflectance values by the following expression (which is the same as eq. (B6)):

$$\frac{\Delta[L_z(\lambda)]_{ss}}{[L_z(\lambda)]_{bw}} = \frac{\{\Delta[\rho_u(\lambda)]_{ss}/[\rho_u(\lambda)]_{bw}\}}{1 + \dfrac{C}{B}} \tag{2}$$

The reflectance ratio $\Delta[\rho_u(\lambda)]_{ss}/[\rho_u(\lambda)]_{bw}$ shown in figure 8 has been computed from values in figure 6. From these curves, it is concluded that differences in both reflectance magnitude and spectral variation occur for different turbid background waters. It is reasonable to expect that the ratio of the difference in apparent radiance to the background-water apparent radiance will also vary for turbid background waters.

The third algorithm investigated was the parameter for the difference in apparent radiance $\Delta[L_z(\lambda)]_{ss}$. This parameter is related to the difference in inherent reflectance by the following expression (which is the same as eq. (B9)):

$$\Delta[L_z(\lambda)]_{ss} = [T_a(\lambda)][L_{so}(\lambda)]\{\Delta[\rho_u(\lambda)]_{ss}\} \tag{3}$$

Again by use of values from figure 6, the inherent-reflectance difference $\Delta[\rho_u(\lambda)]_{ss}$ has been computed and is shown in figure 9. This figure indicates that the two background waters give differences in magnitude of $\Delta[\rho_u(\lambda)]_{ss}$, but its spectral variation is nearly independent of whether mixture 4 or Back River water is the background water. For this particular pollutant (Southwest Philadelphia Waste Treatment Facility sewage sludge), the spectral variation of $\Delta[\rho_u(\lambda)]_{ss}$ appears to be less sensitive to background-water variations than either $[\rho_u(\lambda)]_{ss}/[\rho_u(\lambda)]_{bw}$ or $\Delta[\rho_u(\lambda)]_{ss}/[\rho_u(\lambda)]_{bw}$.

To further investigate characteristics of the $\Delta[\rho_u(\lambda)]_{ss}$ parameter, computations were made to determine how spectral characteristics of $\Delta[\rho_u(\lambda)]_{ss}$ might change with sewage-sludge concentration. These results are shown in figure 10 for three types of background water based on data from figure 5 and reference 9. The parameter $\Delta[\rho_u(\lambda)]_{ss}^{*}$ is shown for filtered, deionized tap water because laboratory reflectance measurements are not considered valid for clear background water, as discussed in appendix A. In clear water, laboratory spectral measurements are not usable unless $\alpha \geq 2$ m^{-1} (concentration of suspended solids usually greater than or equal to 4 ppm). In this case, $\Delta[\rho_u(\lambda)]_{ss}^{*}$ is used to illustrate changes which occur as sewage-sludge

concentration increases from 4 to 69 ppm, whereas $\Delta[\rho_u(\lambda)]_{ss}$ is used to study changes as sludge concentration increases from 0 to 69 ppm. Figure 10 shows a nearly uniform spectrum for both $\Delta[\rho_u(\lambda)]_{ss}$ and $\Delta[\rho_u(\lambda)]^*_{ss}$ for sludge concentrations between 4 and 69 ppm for all three types of background water. The small variations evident in some curves are within the standard deviation of laboratory reflectance values ($\sigma = \pm0.16$ percent).

Knowledge of atmospheric effects is required to relate surface-reflectance to apparent-radiance parameters. Equation (3) shows that values of atmospheric transmission $T_a(\lambda)$ and diffuse-reflector radiance $L_{so}(\lambda)$ are required to convert the difference in inherent reflectance at the water surface $\Delta[\rho_u(\lambda)]_{ss}$ to the difference in radiance at altitude $\Delta[L_z(\lambda)]_{ss}$. Typical values for $T_a(\lambda)$ and $L_{so}(\lambda)$ are shown in figure 11. Figure 11(a) is based on $L_{so}(\lambda)$ measurements made on the beach at Cape Henelopen, Delaware, on July 24, 1978, at 9:40 a.m. EDT. Original measurements were made with a spectrometer at a spectral resolution equal to 16 nm. The values shown in figure 11(a) are integrated average values which simulate each band of the M^2S instrument. Values for $T_a(\lambda)$ were computed every 6 nm by use of the analytical model described in reference 12. Likewise, the values shown in figure 11(b) are integrated averages which simulate the spectral resolution of the M^2S instrument. Figures 11(a) and 11(b) show that $L_{so}(\lambda)$ and $T_a(\lambda)$ typically have different spectral variations. This means that $\Delta[L_z(\lambda)]_{ss}$ will have different spectral characteristics than $\Delta[\rho_u(\lambda)]_{ss}$, as shown in figure 12. Figure 12(a) shows laboratory values of $\Delta[\rho_u(\lambda)]_{ss}$ taken directly from figure 10(b). Calculated values of $\Delta[L_z(\lambda)]_{ss}$ are shown in figure 12(b). Values for $L_{so}(\lambda)$ and $T_a(\lambda)$ from figure 11 were used in equation (3) to obtain $\Delta[L_z(\lambda)]_{ss}$. The standard deviation shown for $\Delta[L_z(\lambda)]_{ss}$ is based on the σ value for $\Delta[\rho_u(\lambda)]_{ss}$ multiplied by $T_a(\lambda)$ and $L_{so}(\lambda)$. In the true case, both $T_a(\lambda)$ and $L_{so}(\lambda)$ also contain measurement errors which propagate into $\Delta[L_z(\lambda)]_{ss}$ and increase the actual standard deviation beyond that shown in figure 12(b). From figure 12, it is clear that calculated values of $\Delta[L_z(\lambda)]_{ss}$ contain significant uncertainty because of the inaccuracy of basic radiance measurements and the number of analytical operations which must be performed to obtain quantitative results.

It is of interest to compare $\Delta[L_z(\lambda)]_{ss}$ values calculated from laboratory tests with results from an actual flight experiment. On October 7, 1976, an experiment was conducted off the coast of Delaware in which environmental conditions were similar to those used in the calculations for figure 12. An M^2S instrument was flown at an altitude of 3.1 km over a dump of primary-treated sewage sludge from the Southwest Philadelphia Waste Treatment Facility. Time of overpass was 11:56 a.m. EDT and atmospheric visibility was approximately 15 km. Solar elevation angle was 44°. The flight data from that test contain some noise which is typical of most multispectral scanner instruments. The average standard deviation for bands 1 through 9 is $\pm0.115 \times 10^{-3}$ mW/cm^2-sr-nm for individual pixels representing an area of 9 m by 9 m each. To reduce this noise, new radiance values were calculated for each pixel based on the average of 49 surrounding pixels (a 7-pixel by 7-pixel square). The pixel averaging process reduced the average noise standard deviation from $\pm0.115 \times 10^{-3}$ mW/cm^2-sr-nm to $\pm0.058 \times 10^{-3}$ mW/cm^2-sr-nm. The noise level differed significantly between individual bands.

To obtain $\Delta[L_z(\lambda)]_{SS}$, "averaged" radiance of a pixel in the sewage-sludge plume was subtracted from the "average" radiance of the background water. The standard deviation of $\Delta[L_z(\lambda)]_{SS}$ was estimated as the square root of 2 times the standard deviation of background-water noise for each band. The result of these calculations is shown in figure 13(a). It is not known what the sewage-sludge concentration was in the plume pixel used in these calculations. Figure 13(a) indicates that the uncertainty in the flight data is of the same order of magnitude as that in the $\Delta[L_z(\lambda)]_{SS}$ values calculated from laboratory data (fig. 13(b)). Spectral variation of $\Delta[L_z(\lambda)]_{SS}$ from flight data is similar in both magnitude and shape to the laboratory curves for the lower concentrations of sewage sludge. Inaccuracies in both sets of data make it such that an accurate comparison with firm conclusions is not possible.

CONCLUDING REMARKS

In an effort to improve understanding of the effects of variations in background water on reflectance spectra, laboratory tests have been conducted with various concentrations of sewage sludge diluted with several types of water. Spectral-reflectance characteristics have been obtained and applied to selected data-analysis algorithms which may have potential for pollutant identification. From these results, the following conclusions are made:

1. Reflectance spectra for sewage-sludge mixtures in turbid waters are dependent upon the reflectance of the background water.

2. The ratio of sewage-sludge reflectance to background-water reflectance showed some spectral variation for different turbid background waters.

3. Spectral differences also occurred in the ratio of "delta" reflectance $\Delta[\rho_u(\lambda)]_{SS}$ to background-water reflectance as background water changed. For this reason, caution is suggested when the ratio of the difference in sewage-sludge apparent radiance and background-water apparent radiance to background-water apparent radiance from aircraft or satellite remote-sensing data is used.

4. The difference in reflectance between sewage sludge and background waters did not show major spectral variations with different turbid background waters. Improved knowledge of atmospheric effects is required before laboratory measurements of inherent reflectance can be accurately related to apparent radiance measured from aircraft or satellite remote sensors.

Langley Research Center
National Aeronautics and Space Administration
Hampton, VA 23665
June 12, 1979

APPENDIX A

LABORATORY AND EQUIPMENT

The cylindrical steel water tank has a diameter of 2.5 m and a depth of
3 m. The bottom is concave as illustrated in figure 1. The tank interior
is coated with a black phenolic paint that absorbs 97 percent of incident
radiation over the spectral range of the measurements (400 to 980 nm). For
these experiments, the tank was filled to within 0.3 m of the top with about
11 600 liters of water.

The circulation system was designed to maintain a vertical and horizontal
homogeneous mixture in the tank and to maintain in suspension particles up to
about 70 μm in diameter (specific gravity of 2.6). This particle size corre-
sponds to fine sand. In order to accomplish these design goals, water is
pumped from the drain at the bottom of the tank into a system of pipes which
returns the water to the tank through two vertical pipes on opposite sides of
the tank. The pipes empty just above the concave bottom. Water entering the
tank through these pipes washes over the concave bottom, meets at a location
away from the drain, and wells upward. Tests using tracer techniques and
transmission measurements have confirmed that this circulation system provides
a nearly uniform homogeneous mixture throughout the tank. For pollutants such
as sewage sludge with specific gravities less than 2.6, the present laboratory
setup can suspend particles larger than 70 μm in diameter.

The filtration and deionization system includes a commercial fiber
swimming-pool filter, an activated carbon filter, and a charged resin
deionizer. These units were placed in water lines parallel to the main cir-
culation system water lines and can be used separately or in any combination
by using valves. The two filters remove particulates and dissolved organic
materials from the water before it reaches the deionizer, where dissolved ionic
substances are removed. After tap water is conditioned through this system, it
contains less than 0.5 ppm of suspended solids and less than 2 ppm of dissolved
substances.

The light source is a solar-radiation simulator designed to approximate
the spectral content of the Sun's rays. The radiation spectrum is produced by
a 2.5-kW xenon short-arc lamp and transferred to the target plane through an
optical arrangement inside the simulator and a collimating lens accessory.
With the collimating lens accessory, the projected beam is collimated to a
0.15-m diameter at 0.3 m from the simulator and has a ±2.5° collimation angle.
For these experiments, the simulator was located approximately 6.0 m from the
water tank (fig. 1). At this distance from the simulator, the beam is about
0.57 m in diameter. A mirror positioned 1.52 m above the water tank reflects
the center of the beam to the water surface. The incidence angle with the
water surface is 13° to avoid specular reflectance. The mirror is a first-
surface mirror coated with aluminum and protected by an overcoat of silicon
monoxide. It has a 0.3-m diameter and reflects an elliptical spot on the water
surface which has a maximum diameter of 0.35 m. The simulator spectral input
to the water surface is similar to, but not a precise duplicate of, sea-level
standard solar-radiation curves often used in engineering calculations

(ref. 13). Figure 2(a) shows that the standard sea-level curves are rather variable, depending on the solar elevation angle. Figure 2(b) shows the simulator spectrum normalized to the solar spectrum at 600 nm and a solar elevation angle of 30°. These curves suggest that when laboratory measurements are made at a 32-nm spectral resolution, the input spectrum and possibly the output measurements are similar to those that would be expected in the field for a solar elevation angle on the order of 30°. The total intensity of the light hitting the water surface is approximately 8 percent of that in actual field conditions.

The rapid-scanning spectrometer system consists of a spectrometer unit with a telephoto lens attachment and a plug-in unit with an oscilloscope and camera attachment. The spectrometer unit with telephoto lens attachment is mounted 2.43 m above the surface of the water (fig. 1). The spectrometer uses a Czerny-Turner grating monochromator without an exit slit. The spectral output of the monochromator is focused on the target of a vidicon tube, where the spectrum is stored as an electrical charge image. An electron beam periodically scans the vidicon target to convert the charge image into an electronic signal. This signal is processed by the plug-in unit, which also functions as a controller between the spectrometer and the oscilloscope. The signal is displayed on the oscilloscope and is photographically recorded with a camera. The spectrometer is designed to measure power per spectral bandwidth (spectral power). The oscilloscope screen is used to show displacement of the instrument measurement. Oscilloscope displacement is proportional to spectral power as shown in the equation

$$D = \frac{P(\lambda)}{S} \tag{A1}$$

The signal is internally processed in such a manner that the vertical-scale sensitivity factor S has a constant value over the wavelength range from 400 to 980 nm. Values of S were obtained by the manufacturer using calibration procedures described in reference 14. (After receipt of the instrument, the manufacturer's calibration was checked in an approximate manner prior to the tests described herein.) The upwelled spectral radiance $L_u(\lambda)$ is defined as

$$L_u(\lambda) = \frac{P(\lambda)}{A\Omega} \tag{A2}$$

where A is the area of the spectrometer entrance slit and Ω is the acceptance solid angle of the spectrometer. Radiance values given herein are based on power received at the detector and are not corrected for losses through the telephoto lens. Tests with and without the lens indicate that such losses are much less than 5 percent for wavelengths between 400 and 980 nm.

Combining equations (A1) and (A2) results in

$$L_u(\lambda) = \frac{DS}{A\Omega} \tag{A3}$$

or

$$L_u(\lambda) = \frac{D}{K} \qquad (A4)$$

where

$$K = \frac{A\Omega}{S}$$

Thus, upwelled spectral radiance is determined from oscilloscope displacement and the proportionality constant K, which is a function of the calibration factor S (which includes optical transmissivity) as well as acceptance angle Ω and slit area A.

In order to obtain spectral reflectance $\rho_u(\lambda)$, radiance measurements are made of a 99-percent diffuse horizontal reflector near the water surface $L_{so}(\lambda)$. Values obtained are proportional to the spectrum being input to the water by the solar simulator. Reflectance is then computed by using the following equation:

$$\rho_u(\lambda) = \frac{[L_u(\lambda)]}{L_{so}(\lambda)} \qquad (A5)$$

By adjusting the slit area, spectral resolution of the spectrometer may be changed. For the tests described herein, all laboratory measurements were made with a spectral resolution of 32 nm.

The instrument has been observed to experience daily variations in the calibration factor K, which affects absolute accuracy. According to instrument specifications, absolute accuracy of the measurements is believed to be ±20 percent in the 400- to 600-nm range and ±12 percent in the 600- to 900-nm range. (A comparison of results from a number of laboratory tests at Langley Research Center tends to verify the manufacturer's specifications.) Included in the absolute error is a repeatability uncertainty of ±13 percent in the 400- to 600-nm range and ±3.5 percent in the 600- to 900-nm range. Discussions with the manufacturer indicate that these values are believed to be representative of 3σ error bands. Because of these absolute errors, spectral radiances from tests conducted on different days usually differ somewhat in magnitude. However, the overall shape of the relative spectrum over the wavelength range is consistent between tests conducted on different days.

Results from laboratory tests are always limited, because the natural environment is not precisely duplicated. The effects of diffuse skylight, for instance, are not simulated in the laboratory used in this study. (The percent value of diffuse skylight to parallel sunlight varies from day to day in the natural environment.) Calculations with quasi-single-scattering and multiple-scattering optical models (ref. 15) have indicated less than 1 percent difference in inherent reflectance between Sun-only and sky-only cases, however. For

this reason, it is believed that inherent-reflectance spectra measured in the laboratory are characteristic of those in the natural environment for the same water mixture.

Measurements of upwelled radiance for clear waters in this laboratory are not considered valid. Data tabulated in reference 16 suggest that beam attenuation coefficient α should have a minimum value of 2.0 m^{-1} before bottom reflection can be ignored when water depth equals 3.0 m. Reference 17 examined the effects of solar spot size and concluded that α should have minimum values between 2.0 and 4.0 m^{-1} to eliminate losses in signal when spot diameter is 0.3 m. The only data that should be considered valid from this laboratory are those for turbid water mixtures with α greater than 2.0 m^{-1}.

APPENDIX B

RELATION OF ALTITUDE RADIANCE TO SURFACE REFLECTANCE

From reference 18, reflectance at sea level and upwelled radiance at an altitude are related as follows:

$$L_z(\lambda) = [T_a(\lambda)]\{[\rho_u(\lambda)][L_{so}(\lambda)] + L_{rd}(\lambda) + L_{rs}(\lambda)\} + L_a(\lambda) \tag{B1}$$

where

$L_z(\lambda)$ apparent upwelled radiance at altitude z, mW/cm^2-sr-nm

$T_a(\lambda)$ atmospheric transmission fraction

$\rho_u(\lambda)$ inherent upwelled spectral reflectance above water surface, percent of input (relative to a 100-percent diffuse reflector)

$L_{so}(\lambda)$ upwelled radiance above water surface from a 100-percent diffuse reflector, mW/cm^2-sr-nm

$L_{rd}(\lambda)$ upwelled radiance from specular reflection of diffuse skylight, mW/cm^2-sr-nm

$L_{rs}(\lambda)$ upwelled radiance from specular reflection of sunlight, mW/cm^2-sr-nm

$L_a(\lambda)$ upwelled radiance from light scattered into receiver by the atmosphere, mW/cm^2-sr-nm

Atmospheric transmission $T_a(\lambda)$ is a function of atmospheric constituents, altitude, and remote-sensor pointing angle (ref. 14); $L_a(\lambda)$ is a function not only of atmospheric constituents and solar elevation angle, but also of target and background reflectance (ref. 19); $L_{so}(\lambda)$ is a function of solar elevation angle and atmospheric conditions; $L_{rd}(\lambda)$ is a function of atmospheric conditions and remote-sensor pointing angle; and $L_{rs}(\lambda)$ is a function of sea state and windspeed in addition to atmospheric and pointing-angle effects (ref. 18). Thus upwelled radiance measured at altitude is a function not only of inherent reflectance of the water but also of altitude, remote-sensor pointing angle, atmospheric constituents, solar elevation angle, sea state, and windspeed.

If the target pollutant and background water are located sufficiently close together and no differences in surface films exist, such that $T_a(\lambda)$, $L_{rd}(\lambda)$, $L_{rs}(\lambda)$, and $L_a(\lambda)$ are equal for both signals, an expression for the ratio of sewage-sludge radiance to background-water radiance can be written

$$\frac{[L_z(\lambda)]_{ss}}{[L_z(\lambda)]_{bw}} = \frac{[T_a(\lambda)]\{[\rho_u(\lambda)]_{ss}[L_{so}(\lambda)] + L_{rd}(\lambda) + L_{rs}(\lambda)\} + L_a(\lambda)}{[T_a(\lambda)]\{[\rho_u(\lambda)]_{bw}[L_{so}(\lambda)] + L_{rd}(\lambda) + L_{rs}(\lambda)\} + L_a(\lambda)} \tag{B2}$$

Rearranging gives

$$\frac{[L_z(\lambda)]_{ss}}{[L_z(\lambda)]_{bw}} = \frac{\{[\rho_u(\lambda)]_{ss}/[\rho_u(\lambda)]_{bw}\}B + C}{B + C} \tag{B3}$$

where

$$B = [L_u(\lambda)]_{bw} = [\rho_u(\lambda)]_{bw}L_{so}(\lambda) \tag{B4}$$

$$C = L_{rd}(\lambda) + L_{rs}(\lambda) + \frac{L_a(\lambda)}{T_a(\lambda)} \tag{B5}$$

Thus, the ratio of sewage-sludge radiance to background-water apparent radiance is a function of altitude, remote-sensor pointing angle, atmospheric constituents, solar elevation angle, sea state, and windspeed, as well as water reflectance ratio.

Another algorithm which has some potential for identification of marine pollutants is one in which the difference between the sewage-sludge radiance and background-water apparent radiance is expressed as a ratio to the apparent radiance of the background water. From equation (B1) this ratio can be expressed as

$$\frac{\Delta[L_z(\lambda)]_{ss}}{[L_z(\lambda)]_{bw}} = \frac{\{\Delta[\rho_u(\lambda)]_{ss}/[\rho_u(\lambda)]_{bw}\}}{1 + \dfrac{C}{B}} \tag{B6}$$

where

$$\Delta[L_z(\lambda)]_{ss} = [L_z(\lambda)]_{ss} - [L_z(\lambda)]_{bw} \tag{B7}$$

$$\Delta[\rho_u(\lambda)]_{ss} = [\rho_u(\lambda)]_{ss} - [\rho_u(\lambda)]_{bw} \tag{B8}$$

This algorithm is similar to that of equation (B3) in that it is a function of altitude, remote-sensor pointing angle, atmospheric constituents, solar elevation angle, sea state, and windspeed, as well as inherent-reflectance characteristics of the water.

A third algorithm often considered for identification of pollutants is the simple difference between the sewage-sludge and background-water apparent radiances as defined in equation (B7). Again assuming that the sewage sludge and background water are located sufficiently close together and no differences in surface films exist such that $T_a(\lambda)$, $L_{rd}(\lambda)$, $L_{rs}(\lambda)$, and $L_a(\lambda)$ are equal for both signals, the algorithm for apparent-radiance difference can be written from equation (B1) as

APPENDIX B

RELATION OF ALTITUDE RADIANCE TO SURFACE REFLECTANCE

From reference 18, reflectance at sea level and upwelled radiance at an altitude are related as follows:

$$L_z(\lambda) = [T_a(\lambda)]\{[\rho_u(\lambda)][L_{so}(\lambda)] + L_{rd}(\lambda) + L_{rs}(\lambda)\} + L_a(\lambda) \tag{B1}$$

where

$L_z(\lambda)$ apparent upwelled radiance at altitude z, $mW/cm^2\text{-}sr\text{-}nm$

$T_a(\lambda)$ atmospheric transmission fraction

$\rho_u(\lambda)$ inherent upwelled spectral reflectance above water surface, percent of input (relative to a 100-percent diffuse reflector)

$L_{so}(\lambda)$ upwelled radiance above water surface from a 100-percent diffuse reflector, $mW/cm^2\text{-}sr\text{-}nm$

$L_{rd}(\lambda)$ upwelled radiance from specular reflection of diffuse skylight, $mW/cm^2\text{-}sr\text{-}nm$

$L_{rs}(\lambda)$ upwelled radiance from specular reflection of sunlight, $mW/cm^2\text{-}sr\text{-}nm$

$L_a(\lambda)$ upwelled radiance from light scattered into receiver by the atmosphere, $mW/cm^2\text{-}sr\text{-}nm$

Atmospheric transmission $T_a(\lambda)$ is a function of atmospheric constituents, altitude, and remote-sensor pointing angle (ref. 14); $L_a(\lambda)$ is a function not only of atmospheric constituents and solar elevation angle, but also of target and background reflectance (ref. 19); $L_{so}(\lambda)$ is a function of solar elevation angle and atmospheric conditions; $L_{rd}(\lambda)$ is a function of atmospheric conditions and remote-sensor pointing angle; and $L_{rs}(\lambda)$ is a function of sea state and windspeed in addition to atmospheric and pointing-angle effects (ref. 18). Thus upwelled radiance measured at altitude is a function not only of inherent reflectance of the water but also of altitude, remote-sensor pointing angle, atmospheric constituents, solar elevation angle, sea state, and windspeed.

If the target pollutant and background water are located sufficiently close together and no differences in surface films exist, such that $T_a(\lambda)$, $L_{rd}(\lambda)$, $L_{rs}(\lambda)$, and $L_a(\lambda)$ are equal for both signals, an expression for the ratio of sewage-sludge radiance to background-water radiance can be written

$$\frac{[L_z(\lambda)]_{ss}}{[L_z(\lambda)]_{bw}} = \frac{[T_a(\lambda)]\{[\rho_u(\lambda)]_{ss}[L_{so}(\lambda)] + L_{rd}(\lambda) + L_{rs}(\lambda)\} + L_a(\lambda)}{[T_a(\lambda)]\{[\rho_u(\lambda)]_{bw}[L_{so}(\lambda)] + L_{rd}(\lambda) + L_{rs}(\lambda)\} + L_a(\lambda)} \tag{B2}$$

13

Rearranging gives

$$\frac{[L_z(\lambda)]_{ss}}{[L_z(\lambda)]_{bw}} = \frac{\{[\rho_u(\lambda)]_{ss}/[\rho_u(\lambda)]_{bw}\}B + C}{B + C} \tag{B3}$$

where

$$B = [L_u(\lambda)]_{bw} = [\rho_u(\lambda)]_{bw}L_{so}(\lambda) \tag{B4}$$

$$C = L_{rd}(\lambda) + L_{rs}(\lambda) + \frac{L_a(\lambda)}{T_a(\lambda)} \tag{B5}$$

Thus, the ratio of sewage-sludge radiance to background-water apparent radiance is a function of altitude, remote-sensor pointing angle, atmospheric constituents, solar elevation angle, sea state, and windspeed, as well as water reflectance ratio.

Another algorithm which has some potential for identification of marine pollutants is one in which the difference between the sewage-sludge radiance and background-water apparent radiance is expressed as a ratio to the apparent radiance of the background water. From equation (B1) this ratio can be expressed as

$$\frac{\Delta[L_z(\lambda)]_{ss}}{[L_z(\lambda)]_{bw}} = \frac{\{\Delta[\rho_u(\lambda)]_{ss}/[\rho_u(\lambda)]_{bw}\}}{1 + \frac{C}{B}} \tag{B6}$$

where

$$\Delta[L_z(\lambda)]_{ss} = [L_z(\lambda)]_{ss} - [L_z(\lambda)]_{bw} \tag{B7}$$

$$\Delta[\rho_u(\lambda)]_{ss} = [\rho_u(\lambda)]_{ss} - [\rho_u(\lambda)]_{bw} \tag{B8}$$

This algorithm is similar to that of equation (B3) in that it is a function of altitude, remote-sensor pointing angle, atmospheric constituents, solar elevation angle, sea state, and windspeed, as well as inherent-reflectance characteristics of the water.

A third algorithm often considered for identification of pollutants is the simple difference between the sewage-sludge and background-water apparent radiances as defined in equation (B7). Again assuming that the sewage sludge and background water are located sufficiently close together and no differences in surface films exist such that $T_a(\lambda)$, $L_{rd}(\lambda)$, $L_{rs}(\lambda)$, and $L_a(\lambda)$ are equal for both signals, the algorithm for apparent-radiance difference can be written from equation (B1) as

14

$$\Delta [L_z(\lambda)]_{ss} = T_a(\lambda) L_{so}(\lambda) \ \Delta [\rho_u(\lambda)]_{ss} \tag{B9}$$

This algorithm appears to have some advantage over those of equations (B3) and (B6) in that variations due to specular reflection of skylight and sunlight as well as atmospheric backscattering have been eliminated. This means that radiance difference is a function of inherent-reflectance difference, altitude, remote-sensor pointing angle, atmospheric constituents, and solar elevation angle.

REFERENCES

1. Usry, J. W.; and Hall, John B., Jr.: National Aeronautics and Space Administration Operations – Remote Sensing Experiments in the New York Bight, April 7-17, 1975. NASA TM X-72802, 1975.

2. Hypes, Warren D.; and Ohlhorst, Craig W.: A Summary of the Test Procedures and Operational Details of a Delaware River and an Ocean Dumping Pollution Monitoring Experiment Conducted August 28, 1975. NASA TM X-74005, 1977.

3. Johnson, Robert W.; and Hall, John B., Jr.: Remote Sensing Operations (Multispectral Scanner and Photographic) in the New York Bight, September 22, 1975. NASA TM X-73993, 1977.

4. Hypes, W. D.; Wallace, J. W.; and Gurganus, E. A.: A Summary of the Test Procedures and Operational Details of an Ocean Dumping Pollution Monitoring Experiment Conducted October 7, 1976. NASA TM-74066, 1977.

5. Johnson, Robert W.: Multispectral Analysis of Ocean Dumped Materials. NASA paper presented at the Eleventh International Symposium on Remote Sensing of Environment (Ann Arbor, Michigan), Apr. 25-29, 1977.

6. Johnson, R. W.; Duedall, I. W.; Glasgow, R. M.; Proni, J. R.; and Nelsen, T. A.: Quantitative Mapping of Suspended Solids in Wastewater Sludge Plumes in the New York Bight Apex. J. Water Pollut. Control Fed., vol. 49, no. 10, Oct. 1977, pp. 2063-2073.

7. Johnson, Robert W.; Ohlhorst, Craig W.; and Usry, Jimmy W.: Location, Identification, and Mapping of Sewage Sludge and Acid Waste Plumes in the Atlantic Coastal Zones. Conference Proceedings – 4th Joint Conference on Sensing of Environmental Pollutants, American Chem. Soc., c.1978, pp. 644-647.

8. Lewis, Beverley W.; and Collins, Vernon G.: Remotely Sensed and Laboratory Spectral Signatures of an Ocean-Dumped Acid Waste. NASA TN D-8467, 1977.

9. Usry, J. W.; Witte, William G.; Whitlock, Charles H.; and Gurganus, E. A.: Laboratory Measurements of Radiance and Reflectance Spectra of Dilute Primary-Treated Sewage Sludge. NASA TP-1038, 1977.

10. Witte, William G.; Usry, J. W.; Whitlock, Charles H.; and Gurganus, E. A.: Laboratory Measurements of Radiance and Reflectance Spectra of Dilute Secondary-Treated Sewage Sludge. NASA TP-1089, 1977.

11. Methods for Chemical Analysis of Water and Wastes 1971. 16020 - 07/71, Environmental Protection Agency, 1971.

12. Selby, J. E. A.; and McClatchey, R. A.: Atmospheric Transmittance From 0.25 to 28.5 μm: Computer Code LOWTRAN 3. AFCRL-TR-75-0255, U.S. Air Force, May 1975.

16

13. Moon, Parry: Proposed Standard Solar-Radiation Curves for Engineering Use. J. Franklin Inst., vol. 230, no. 5, Nov. 1940, pp. 583-617.

14. Stair, Ralph; Johnston, Russell G.; and Halbach, E. W.: Standard of Spectral Radiance for the Region of 0.25 to 2.6 Microns. J. Res. Natl. Bur. Stand., vol. 64A, no. 4, July-Aug. 1960, pp. 291-296.

15. McCluney, W. R.: Ocean Color Spectrum Calculations. Appl. Opt., vol. 13, no. 10, Oct. 1974, pp. 2422-2429.

16. Whitlock, C. H.: An Estimate of the Influence of Sediment Concentration and Type on Remote Sensing Penetration Depth for Various Coastal Waters. NASA TM X-73906, 1976.

17. Ghovanlou, A.: Radiative Transfer Model for Remote Sensing of Suspended Sediments in Water. NASA CR-145145, 1977.

18. Miller, J. R.; Jain, S. C.; O'Neill, N. T.; McNeil, W. R.; and Thomson, K. P. B.: Interpretation of Airborne Spectral Reflectance Measurements Over Georgian Bay. Remote Sensing Environ., vol. 6, no. 3, 1977, pp. 183-200.

19. Wezernak, C. T.; Turner, R. T.; and Lyzenga, D. R.: Spectral Radiance and Reflectance Characteristics of Water Pollutants. NASA CR-2665, 1976.

TABLE I.- COMPONENTS OF ARTIFICIAL SEAWATER

Sequence of addition	Compound	Amount, grams, added per liter of filtered, deionized tap water
1	NaCl	12.265
2	Na_2SO_4	2.045
3	KCl	.350
4	$NaHCO_3$	.100
5	KBr	.050
6	H_3BO_3	.015
7	$MgCl \cdot 6H_2O$	5.550
8	$SrCl_2 \cdot 6H_2O$	.255
9	$CaCl_2$	.580
10	NaF	.0015

TABLE II.- NUTRIENTS ADDED TO ARTIFICIAL SEAWATER

Compound	Amount, grams, per liter of artificial seawater
KNO_3	0.00600
Na_2HPO_4	.01000
$FeSO_4 \cdot 7H_2O$	.00498
$ZnSO_4 \cdot 7H_2O$	.00882
$MnCl_2 \cdot 4H_2O$	.00144
MoO_3	.00071
$Co(NO_3)_2 \cdot 6H_2O$	.00049
EDTA	.05000
KOH	.03100
H_3BO_3	.01140
$Fe(NH_4)_2(SO_4)_2 \cdot 6H_2O$	.03510
NaEDTA	.03300
Biotin	.00010
B_{12}	.00010
Thiamine HCl	.02000
$Na_2SiO_3 \cdot 9H_2O$	.00466

TABLE III.- RESULTS OF LABORATORY ANALYSIS OF TEST-WATER MIXTURES

Mixture[a]	Description	α, m^{-1}	Suspended solids			Chlorophyll a concentration, µg/ℓ	Algae count, cells/mℓ
			Organic, ppm	Inorganic, ppm	Total, ppm		
1	Artificial seawater plus algae	1.5	3.6	3.4	7.0	7	1.8×10^4
2	Mixture 1 plus algae	2.2	4.7	2.1	6.8	15	3.4
3	Mixture 2 plus algae	2.9	4.6	5.0	9.6	20	4.5
4	Mixture 3 plus overnight growth	7.3	6.2	5.4	11.6	31	6.0
5	Mixture 4 plus sewage sludge	9.2	8.9	10.4	19.3	26	6.5
6	Mixture 5 plus sewage sludge	21.2	20.7	20.0	48.7	27	6.2

[a]Mixture 0 is considered to be artificial seawater plus nutrients.

First-surface mirror

Spectrometer

Enclosure

Solar simulator

Tunnel

Near-parallel light ($\pm 2.5^0$)

.35 m

3.0 m

Absorbent coating (black)

2.5 m

Deionization and filtration system

Circulation system
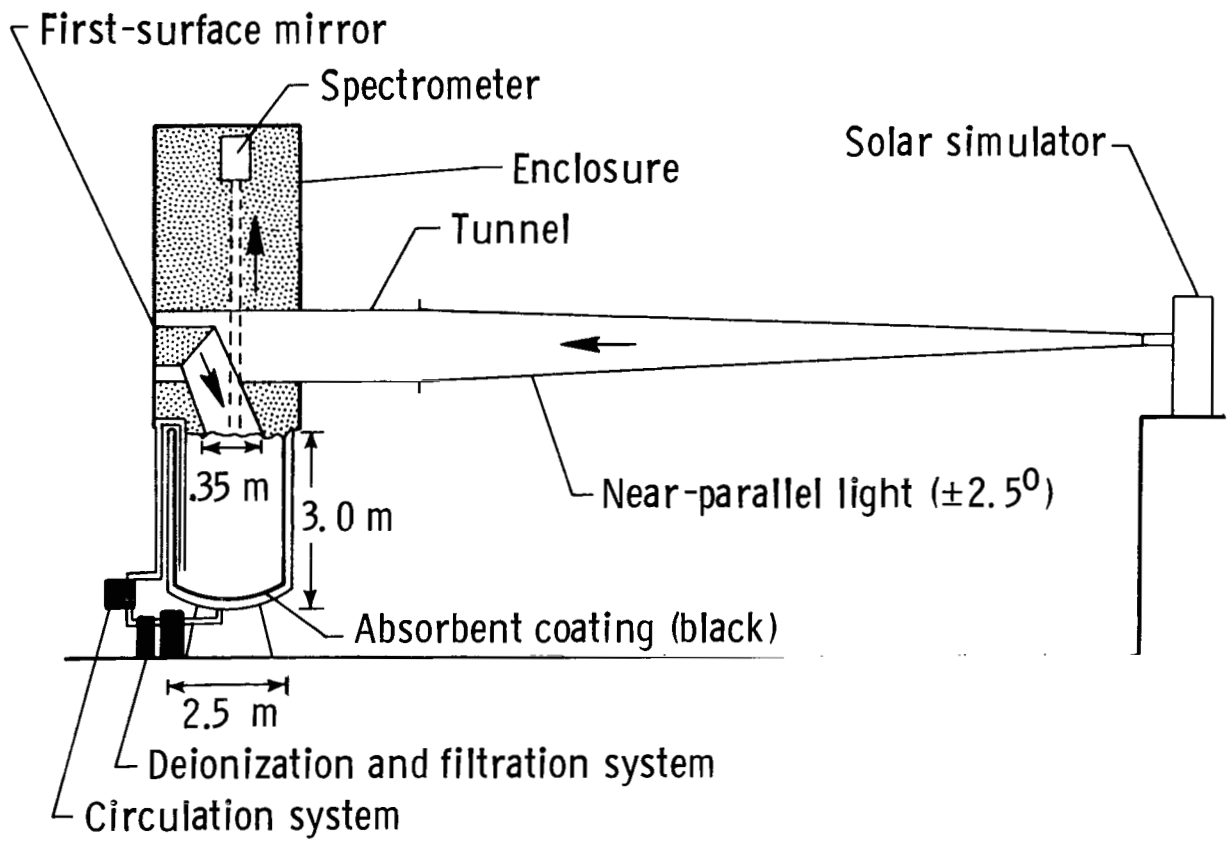
Figure 1.– Sketch of laboratory setup.
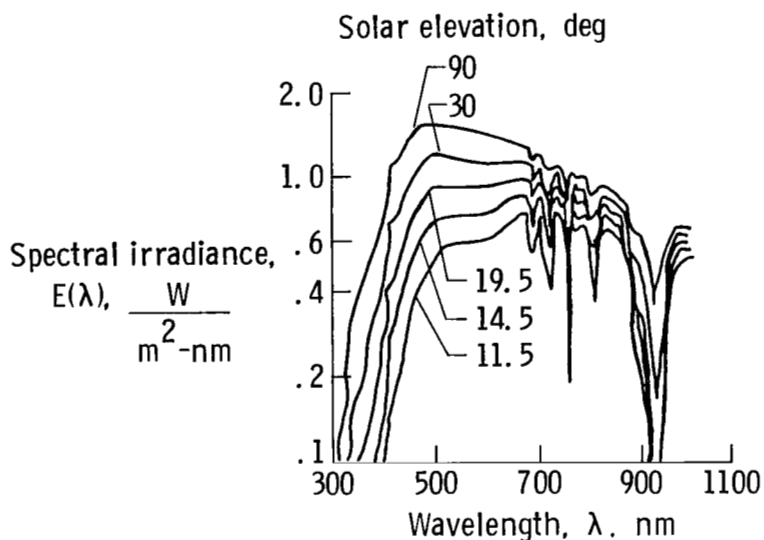
(a) Standard sea-level solar irradiance spectra (ref. 13).

```
------ Solar simulator (32-nm spectral resolution), past tests
– – – Solar simulator (32-nm spectral resolution), present tests
———— Solar elevation, 30°
```
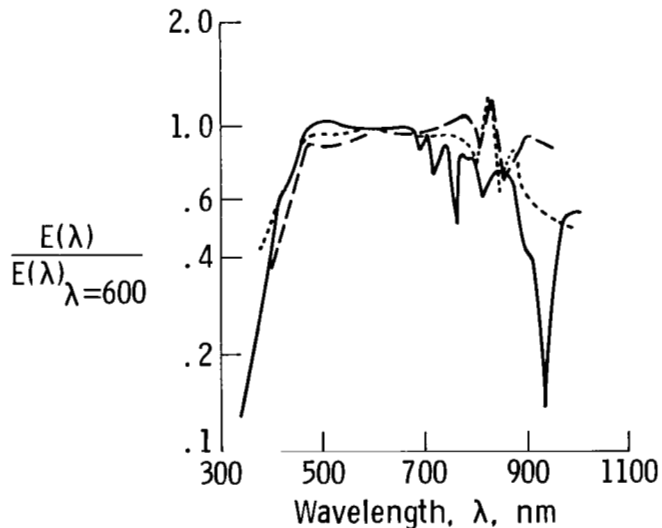

(b) Solar-simulator and standard sea-level spectra.

Figure 2.- Standard sea-level solar irradiance spectra and comparison with solar-simulator data.
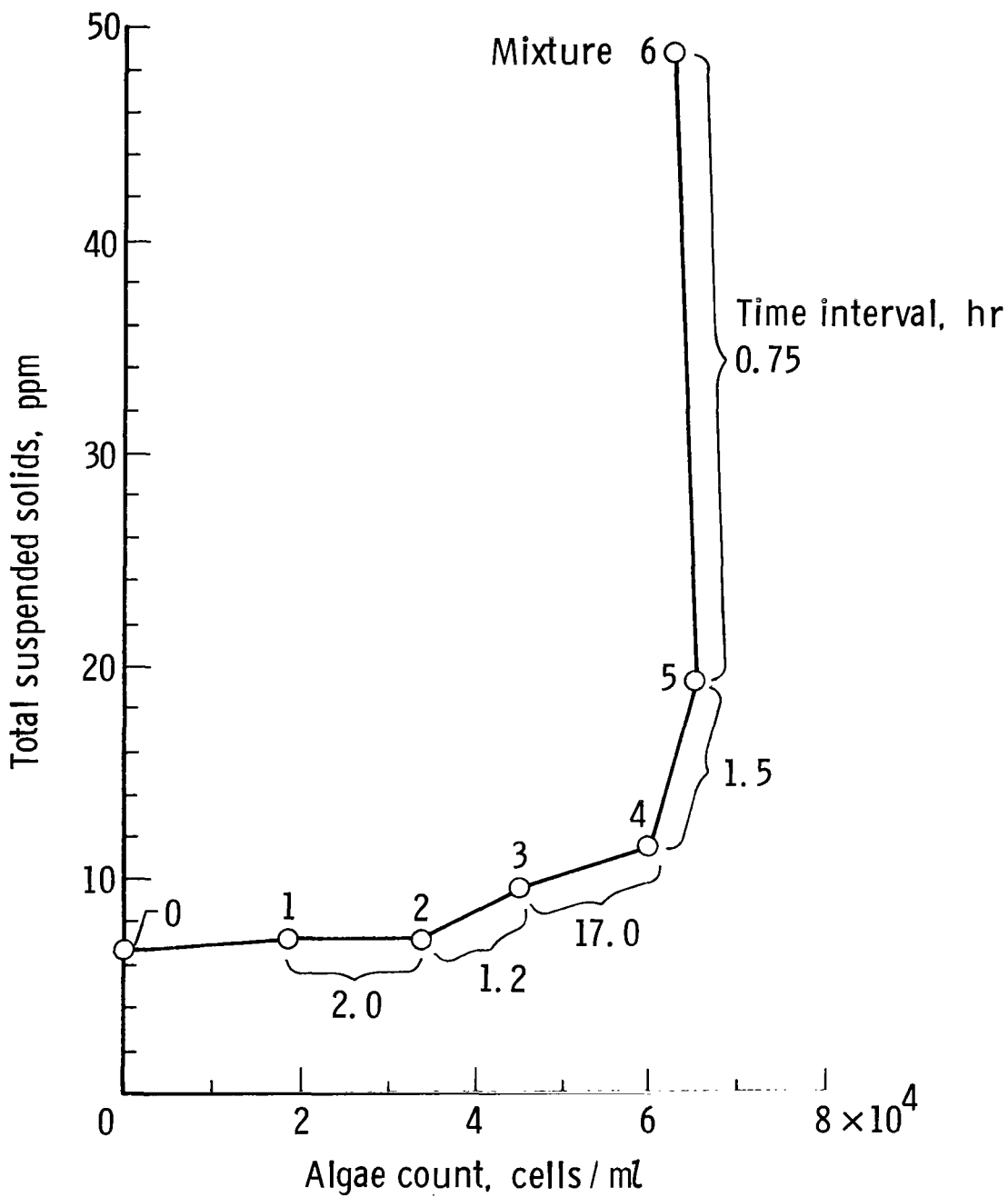
Figure 3.- Laboratory test sequence.
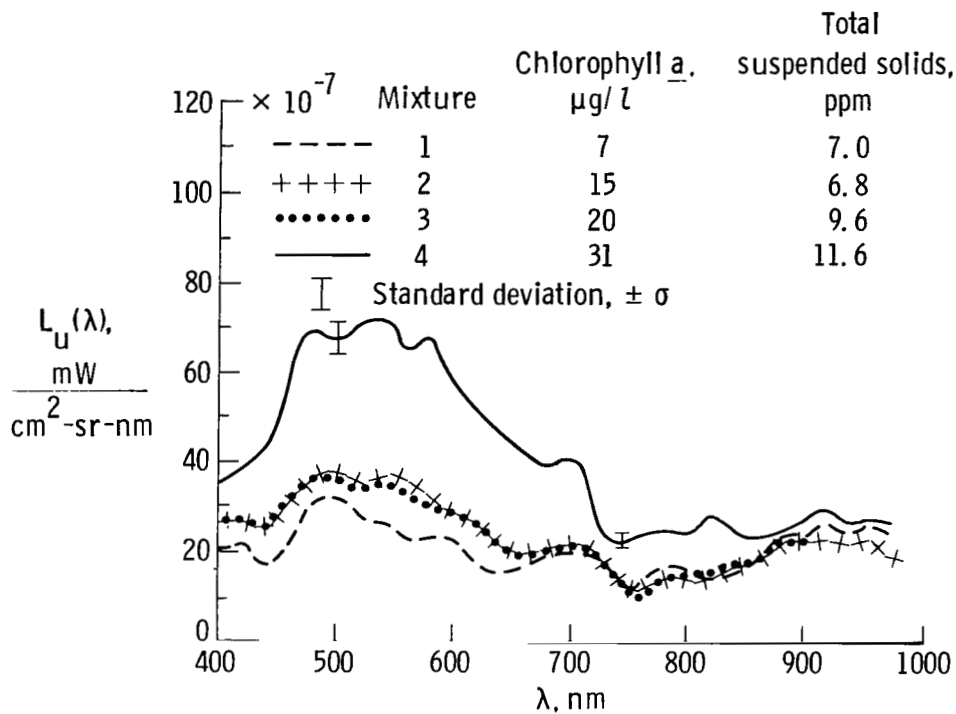
(a) Spectral radiance.
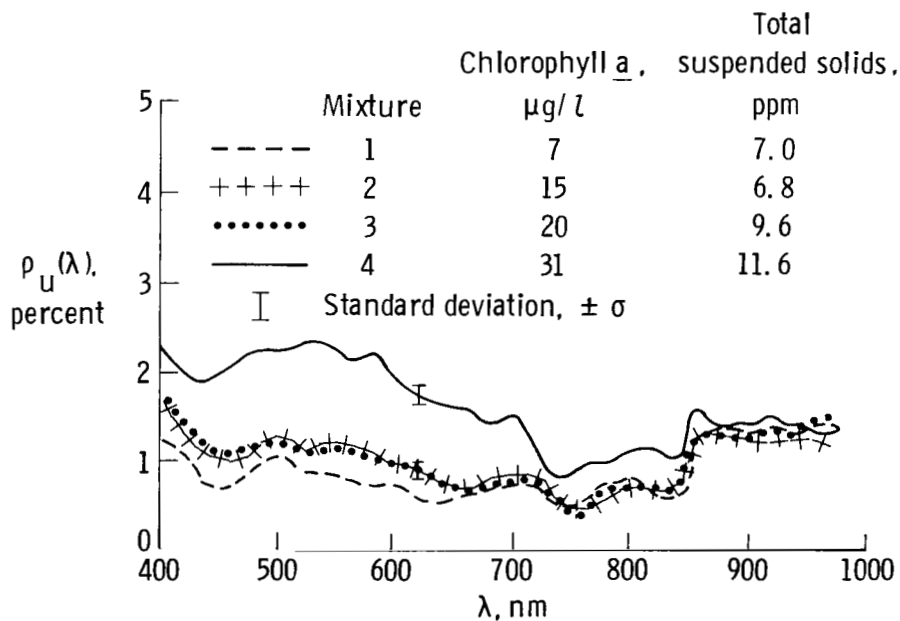
(b) Spectral reflectance.

Figure 4.- Laboratory spectral radiance and reflectance for artificial seawater-algae mixtures. Spectral resolution, 32 nm.

23

Mixture	Chlorophyll a, μg/l	Sewage sludge, ppm	Total, ppm
4	31	0	11.6
5	26	7.7	19.3
6	27	37.1	48.7

Standard deviation, ± σ

$L_u(\lambda)$, $\dfrac{mW}{cm^2\text{-}sr\text{-}nm}$

120 ⎡ × 10^{-7}

100

80   Sewage-sludge mixtures

60

40

20   Background water

0
400   500   600   700   800   900   1000

λ, nm
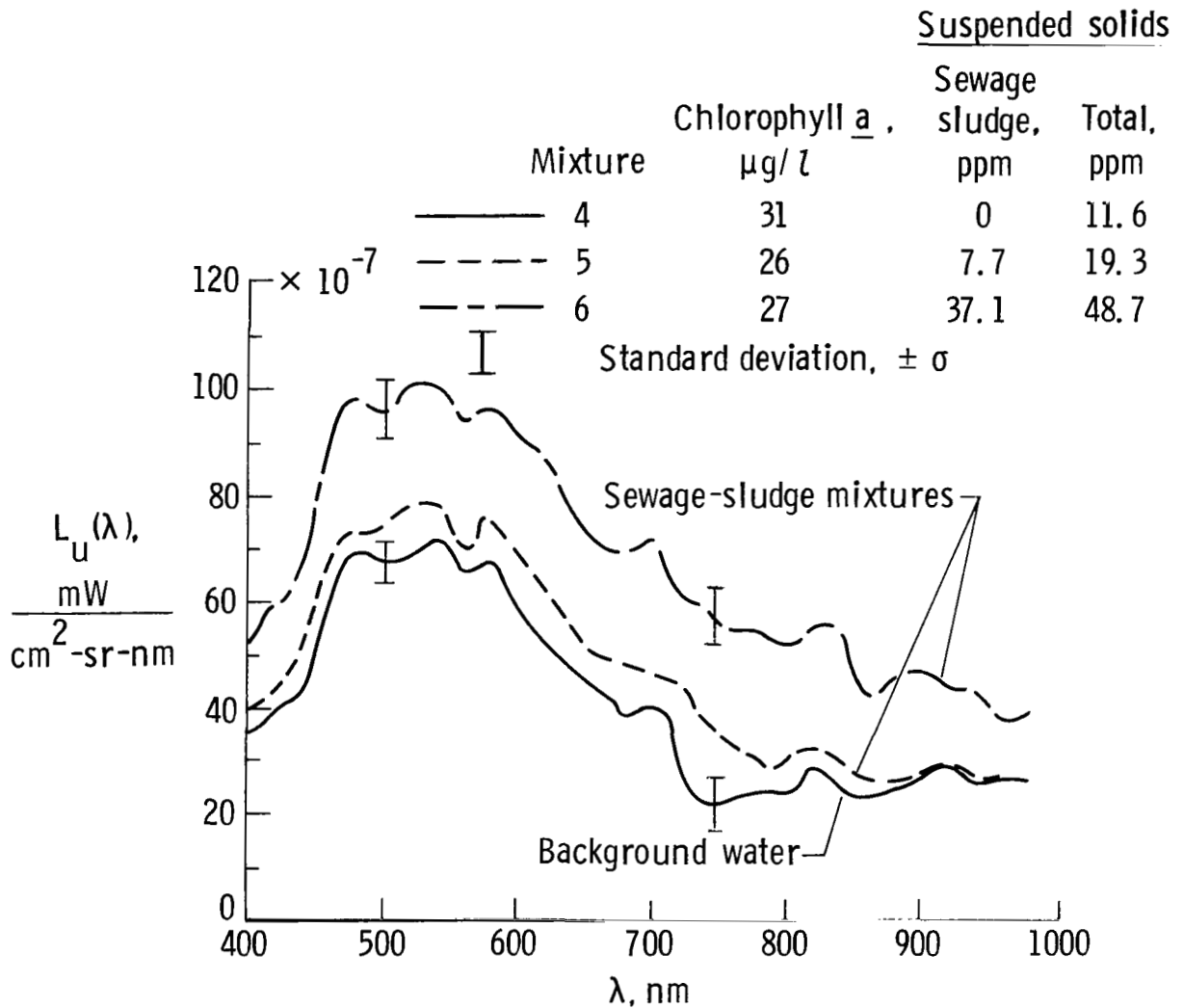
(a) Spectral radiance.

Figure 5.- Laboratory spectral radiance and reflectance for background water and sewage-sludge mixtures. Spectral resolution, 32 nm.

Mixture	Chlorophyll $\underline{a}$, µg/l	Suspended solids	
		Sewage sludge, ppm	Total, ppm
———— 4	31	0	11.6
------- 5	26	7.7	19.3
—·—·— 6	27	37.1	48.7
$\;$ Standard deviation, ± σ			
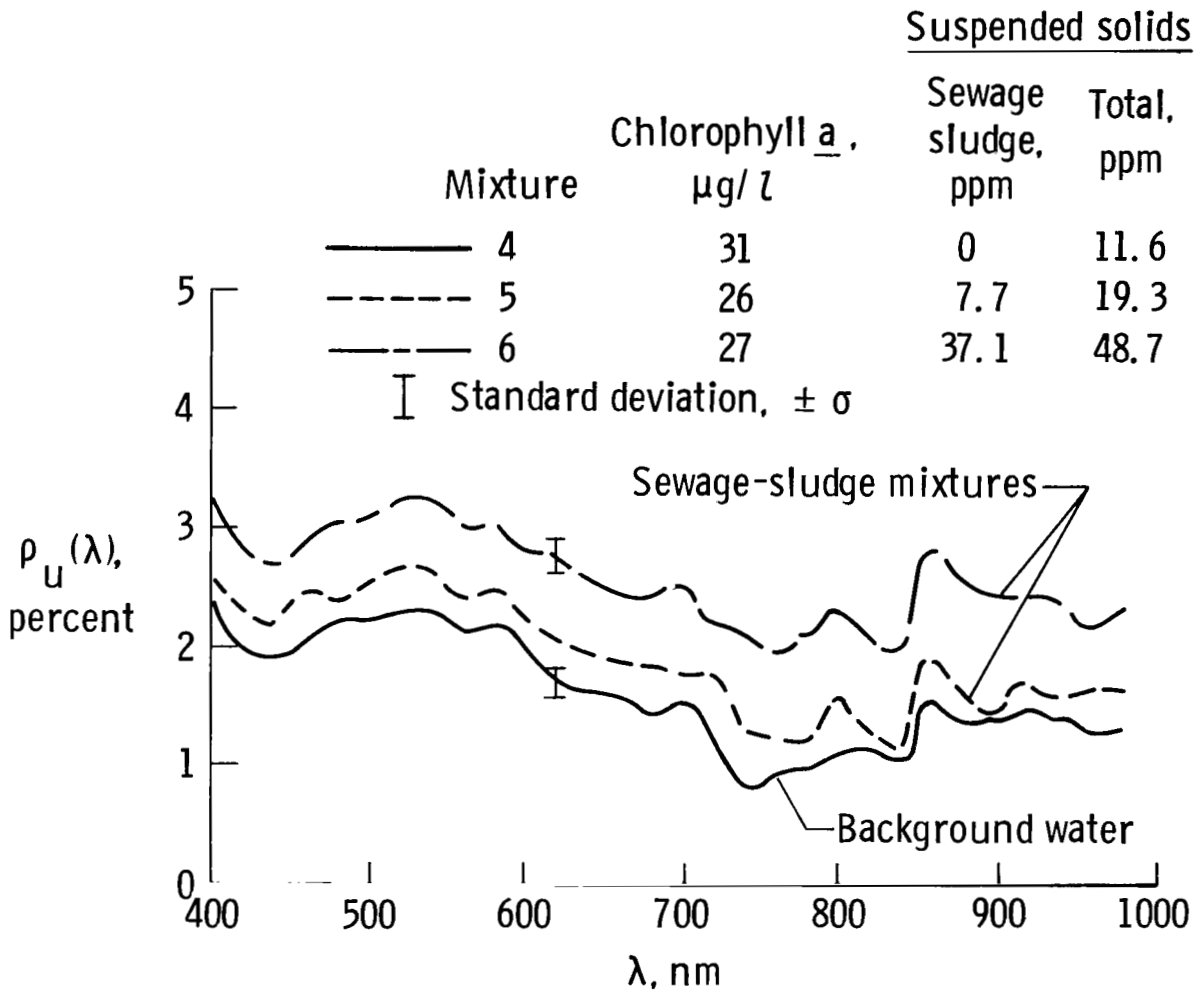
(b) Spectral reflectance.

Figure 5.- Concluded.
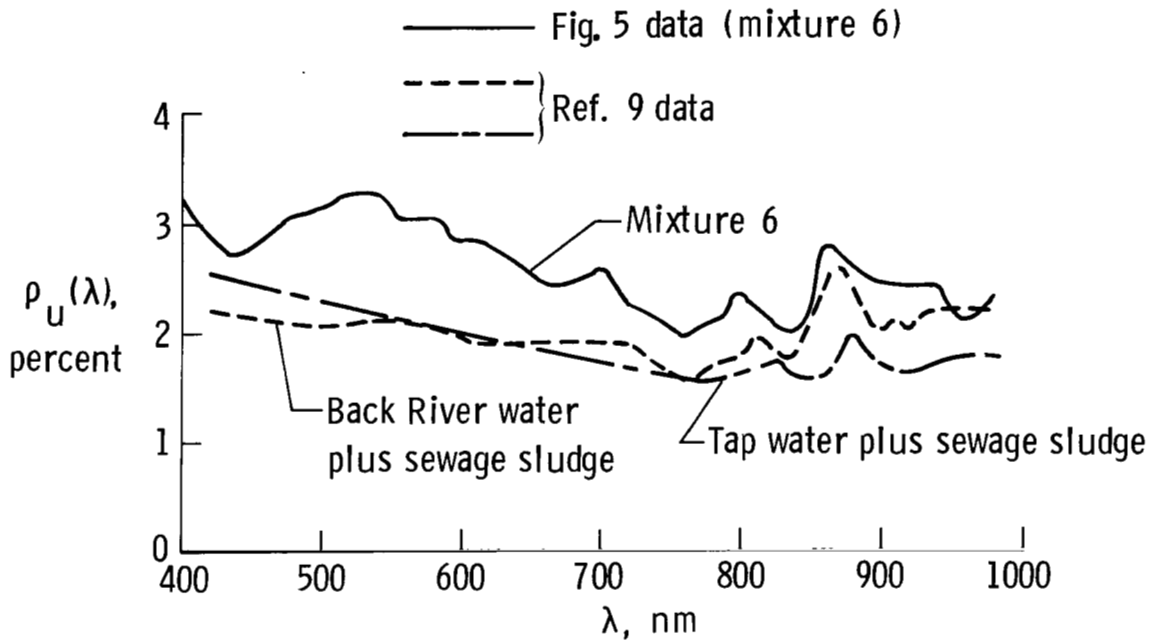
(a) Sewage-sludge mixtures of about 34 ppm.
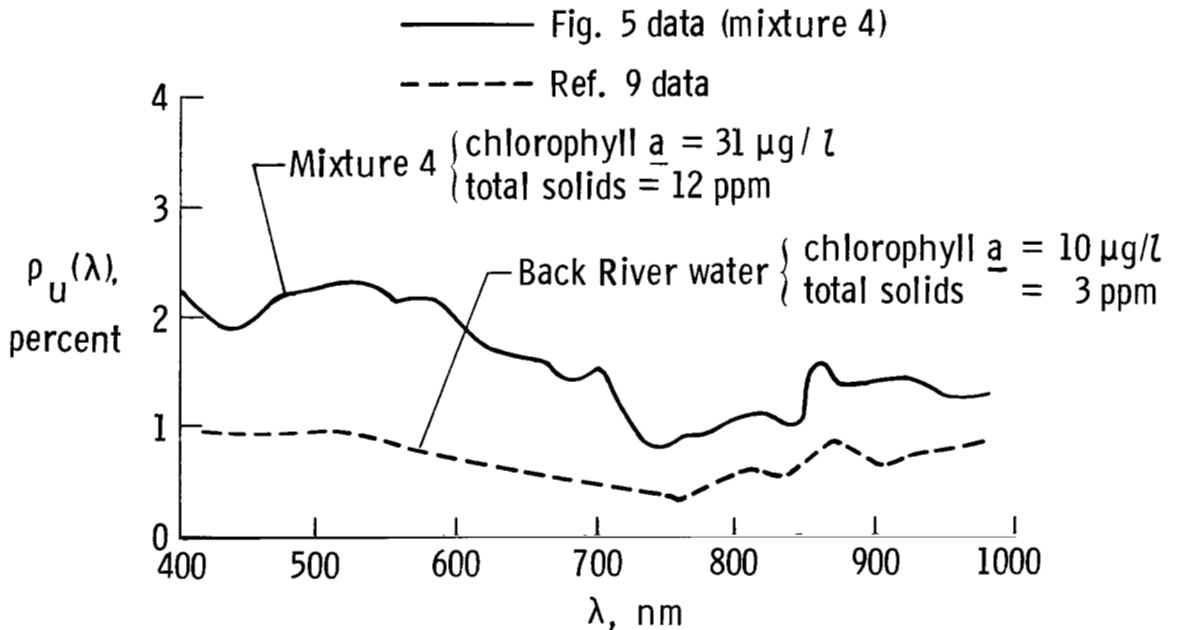
(b) Background water.

Figure 6.- Spectral reflectance of mixture 4, mixture 6, and Back River water. Spectral resolution, 32 nm.
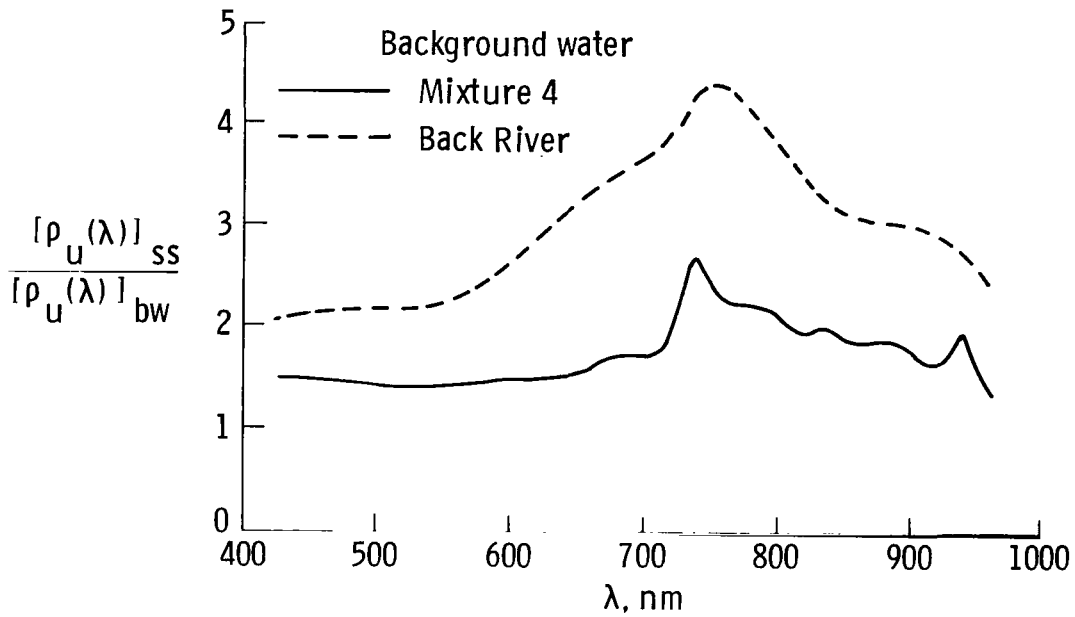
(a) Laboratory-measured spectra. Spectral resolution, 32 nm.
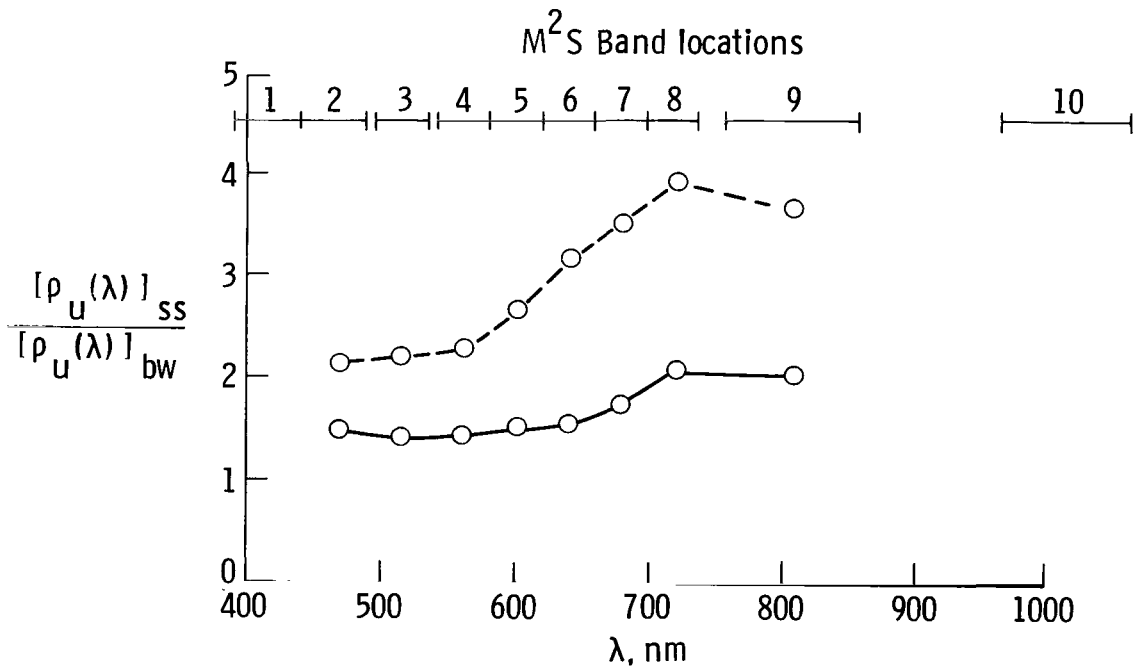
(b) Simulated spectra for M^2S instrument.

Figure 7.- Ratio of sewage-sludge reflectance to background-water reflectance for sewage-sludge concentration of about 34 ppm.
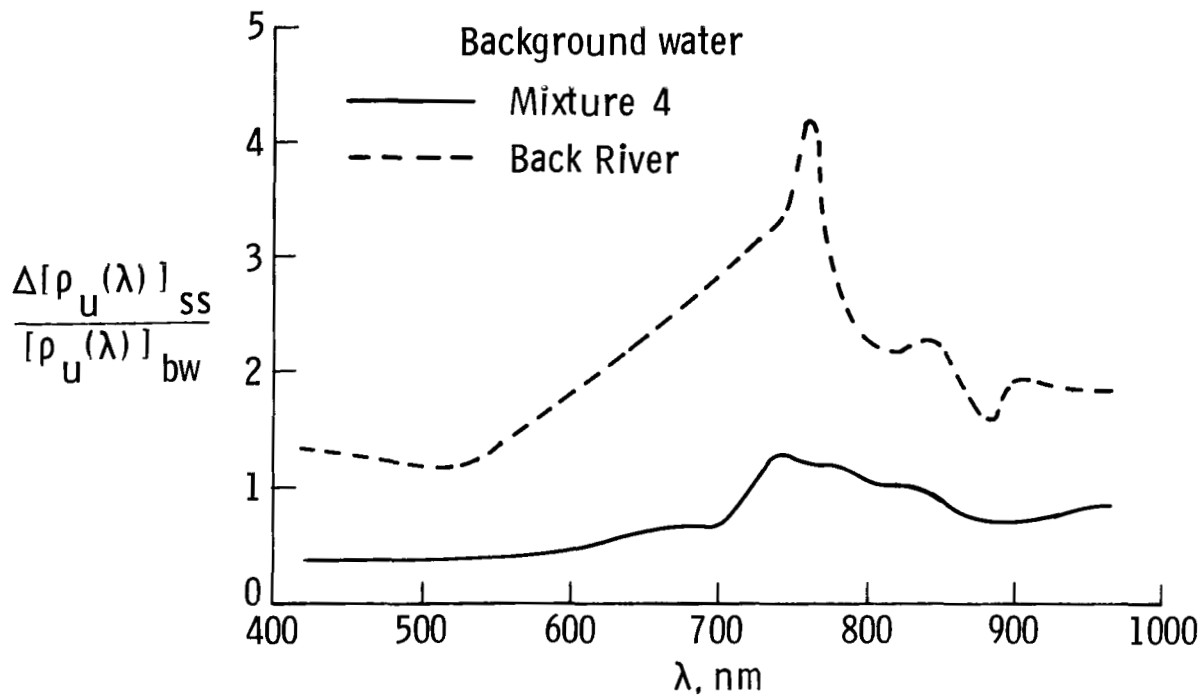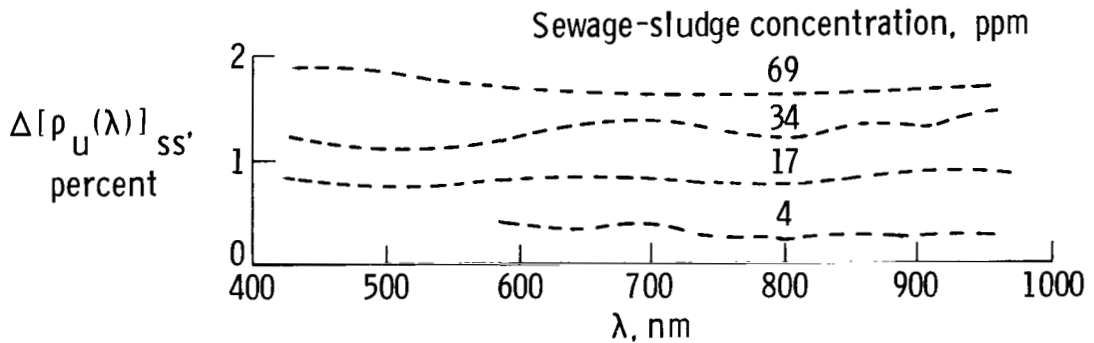
(a) Laboratory-measured spectra.   Spectral resolution, 32 nm.
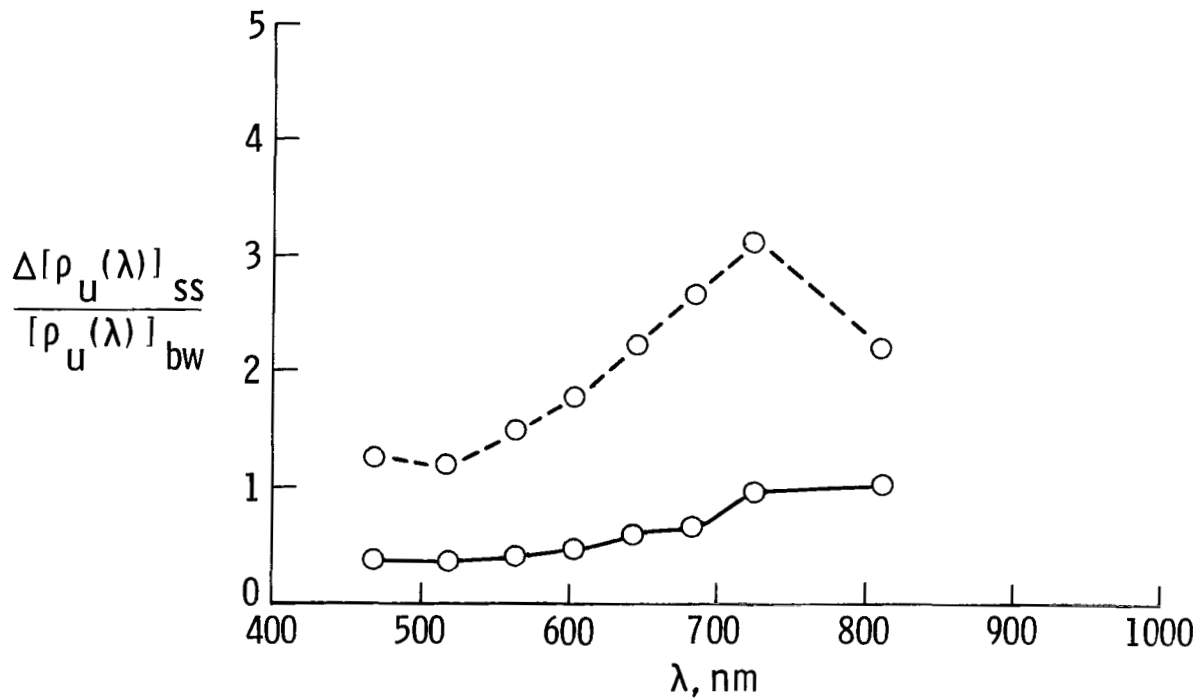
(b) Simulated spectra for M^2S instrument.

Figure 8.- Ratio of difference between sewage-sludge reflectance and
background-water reflectance to background-water reflectance for
sewage-sludge concentration of about 34 ppm.
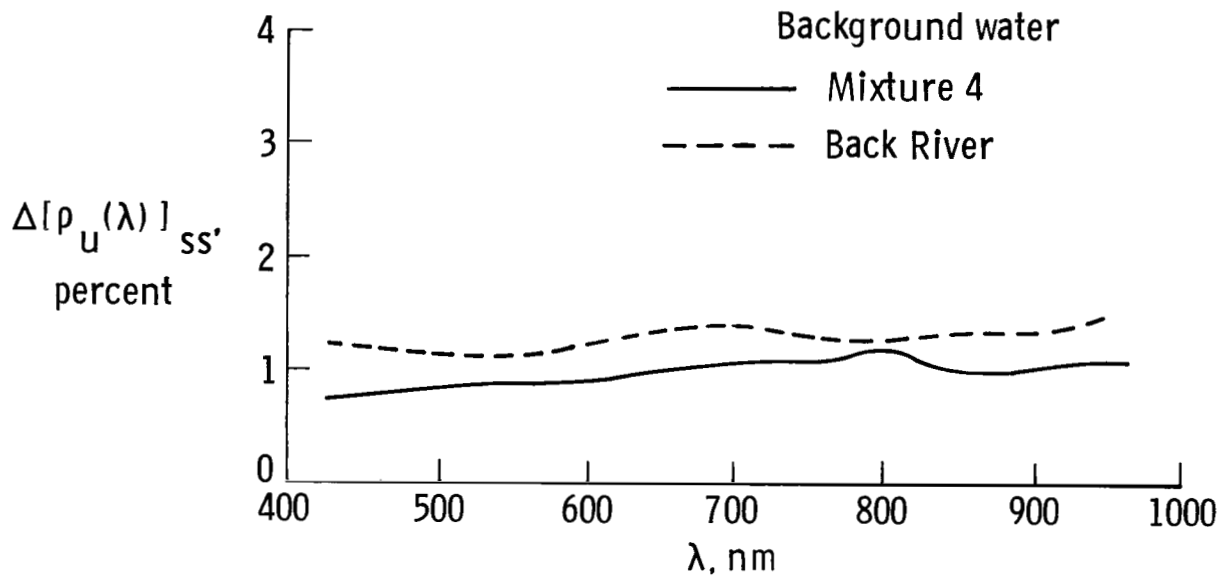
(a) Laboratory-measured spectra.   Spectral resolution, 32 nm.
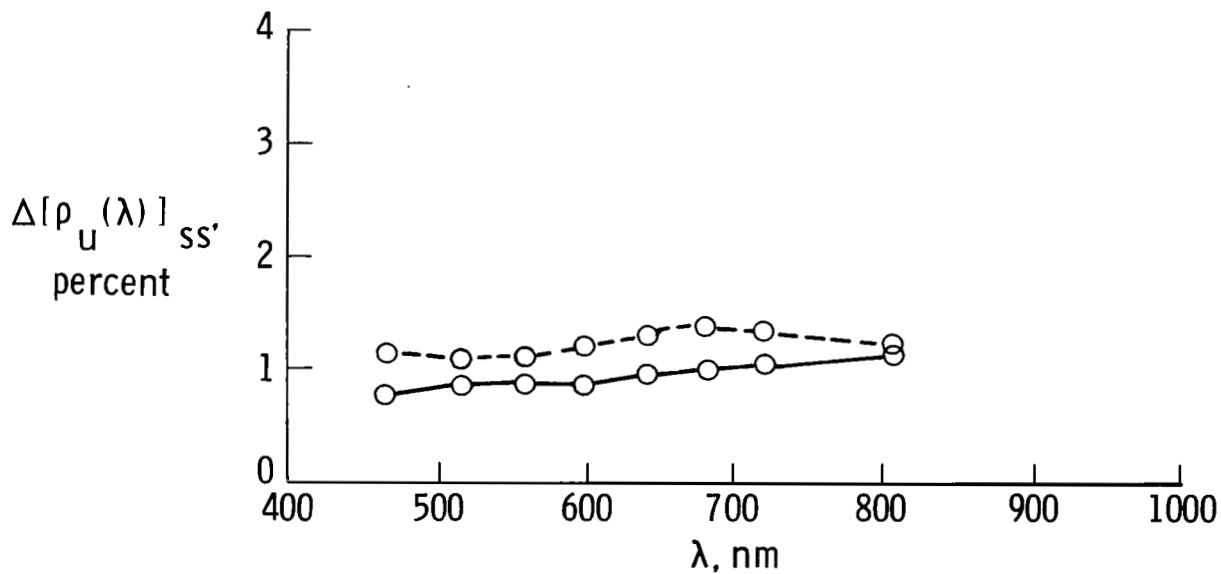
(b) Simulated spectra for M^2S instrument.

Figure 9.- Difference between sewage-sludge reflectance and background-water
reflectance for sewage-sludge concentration of about 34 ppm.

$$\Delta[\rho_u(\lambda)]_{ss} = [\rho_u(\lambda)]_{ss} - [\rho_u(\lambda)]_{bw}$$

$$\Delta[\rho_u(\lambda)]_{ss}^* = [\rho_u(\lambda)]_{ss} - [\rho_u(\lambda)]_{ss} = 4 \text{ ppm}$$

$\Delta[\rho_u(\lambda)]_{ss'}$ percent

Sewage-sludge concentration, ppm

34

8

λ, nm

(a) Mixture 4.

$\Delta[\rho_u(\lambda)]_{ss'}$ percent

Sewage-sludge concentration, ppm

69

34

17

4

λ, nm

(b) Back River water.

$\Delta[\rho_u(\lambda)]_{ss'}^*$ percent

Sewage-sludge concentration, ppm

69

34

17

λ, nm
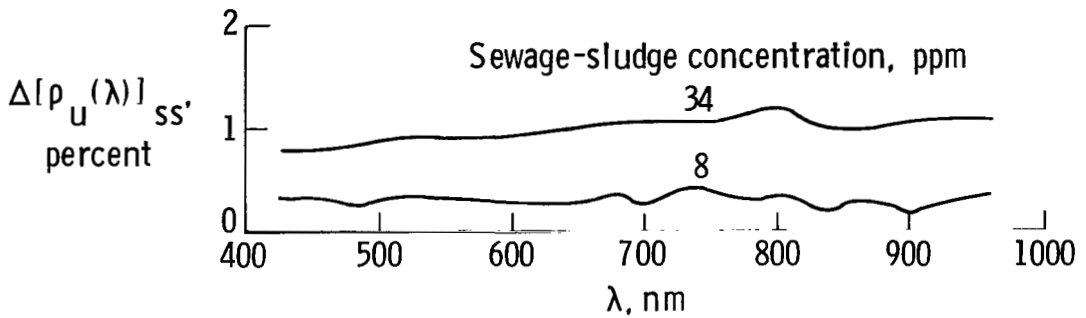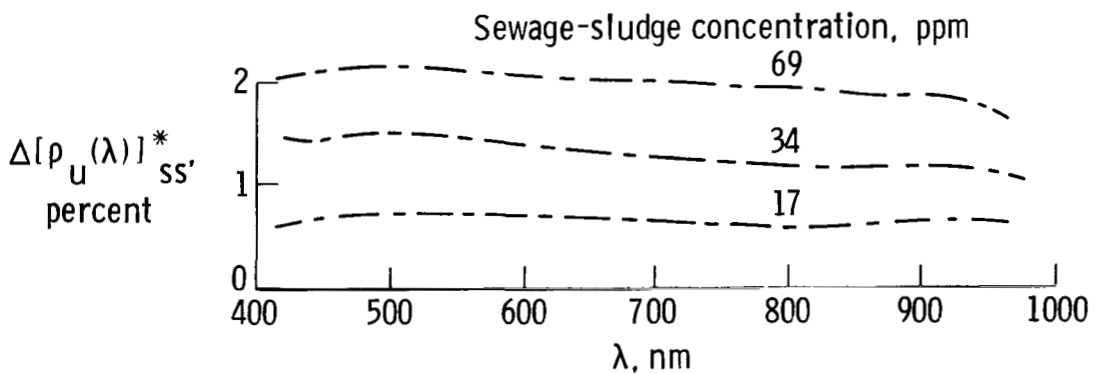
(c) Filtered, deionized tap water.

Figure 10.- Spectra of reflectance differences for several sewage-sludge concentrations in different background waters. Spectral resolution, 32 nm.
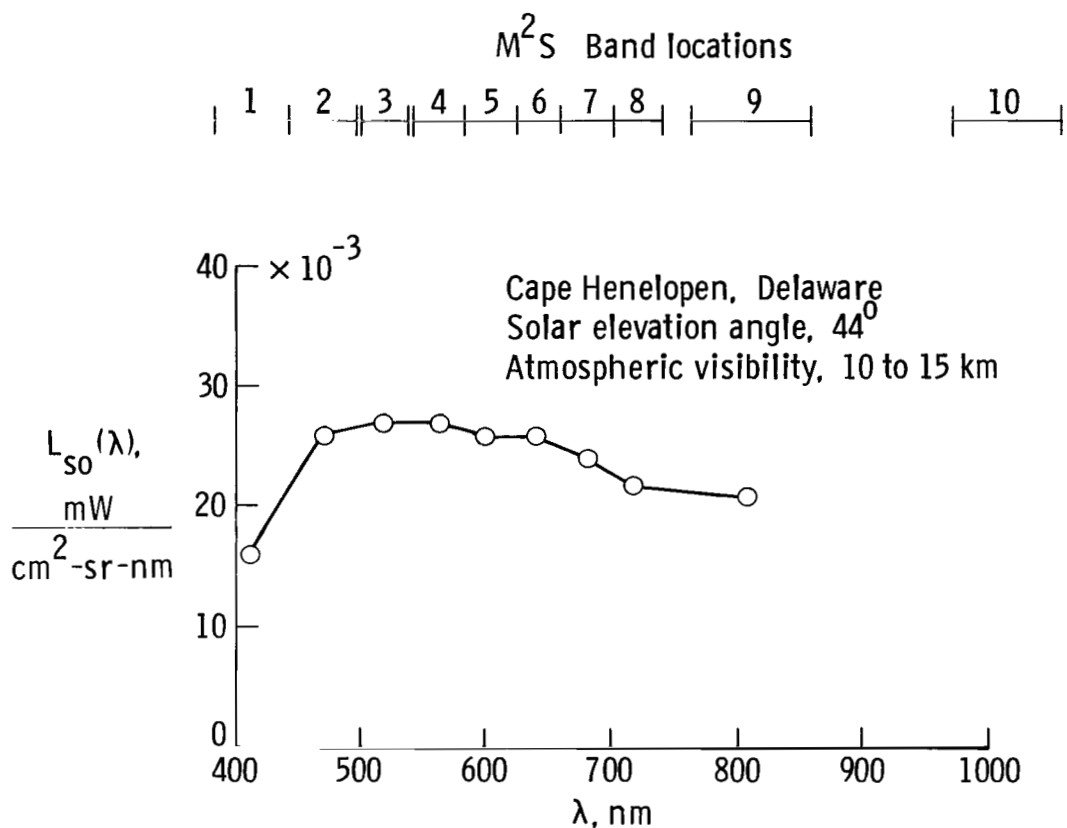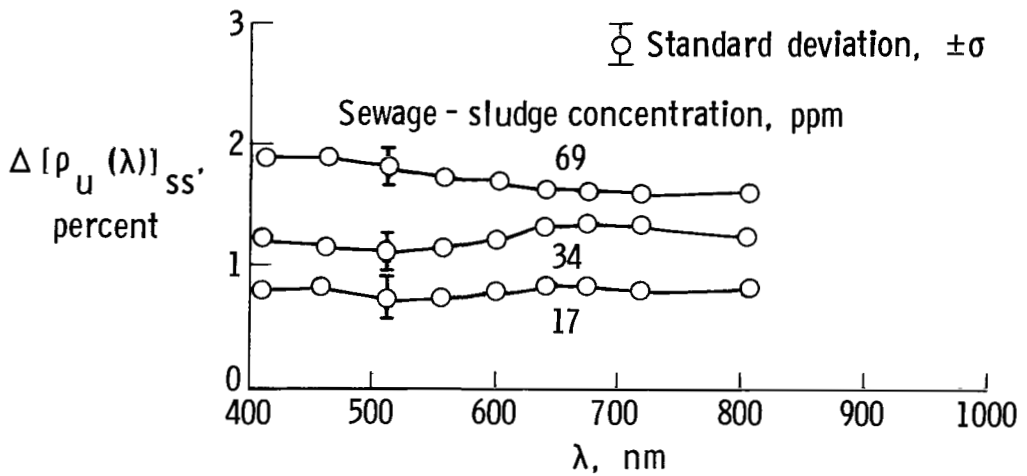
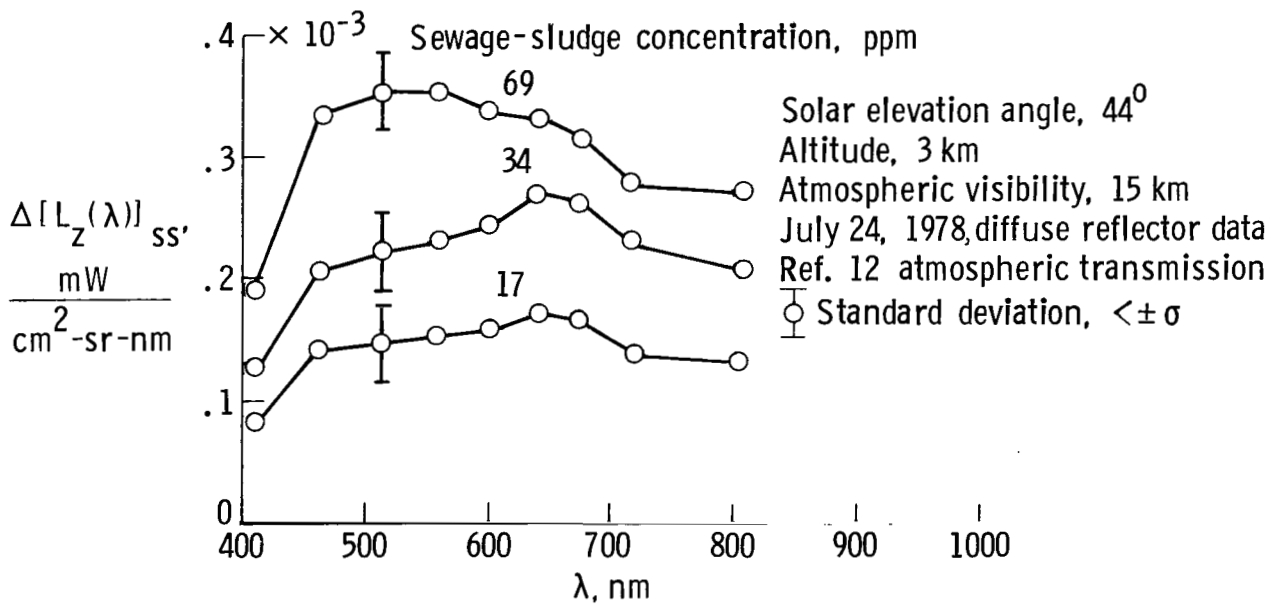(a) Radiance from diffuse reflector measured on July 24, 1978.
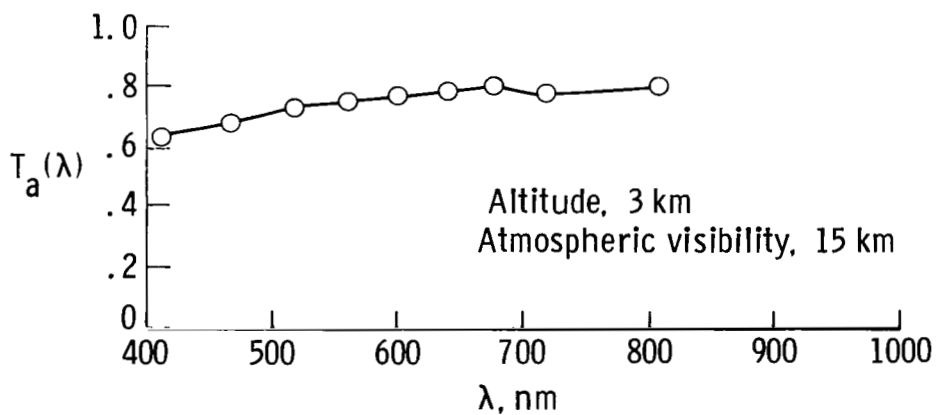
(b) Calculated atmospheric transmission from analytic model of reference 12.

Figure 11.- Typical diffuse-reflector radiance and atmospheric transmission spectra for M^2S instrument bands.
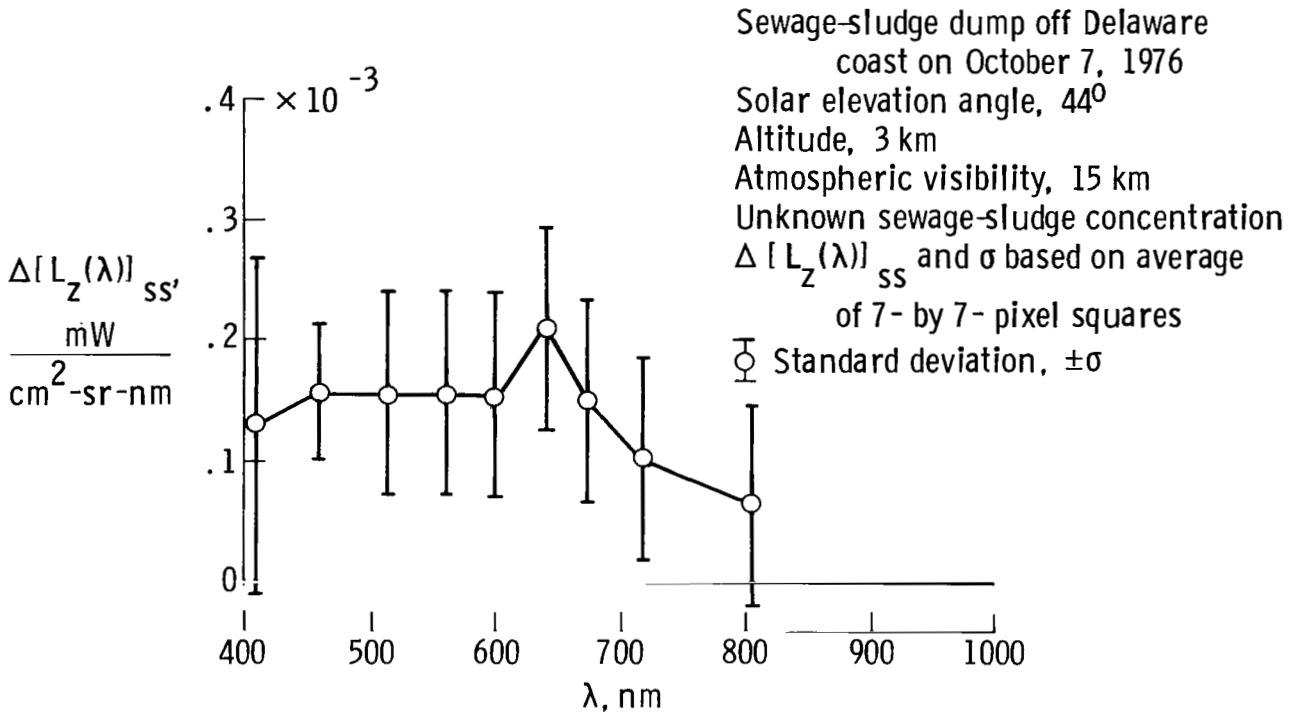
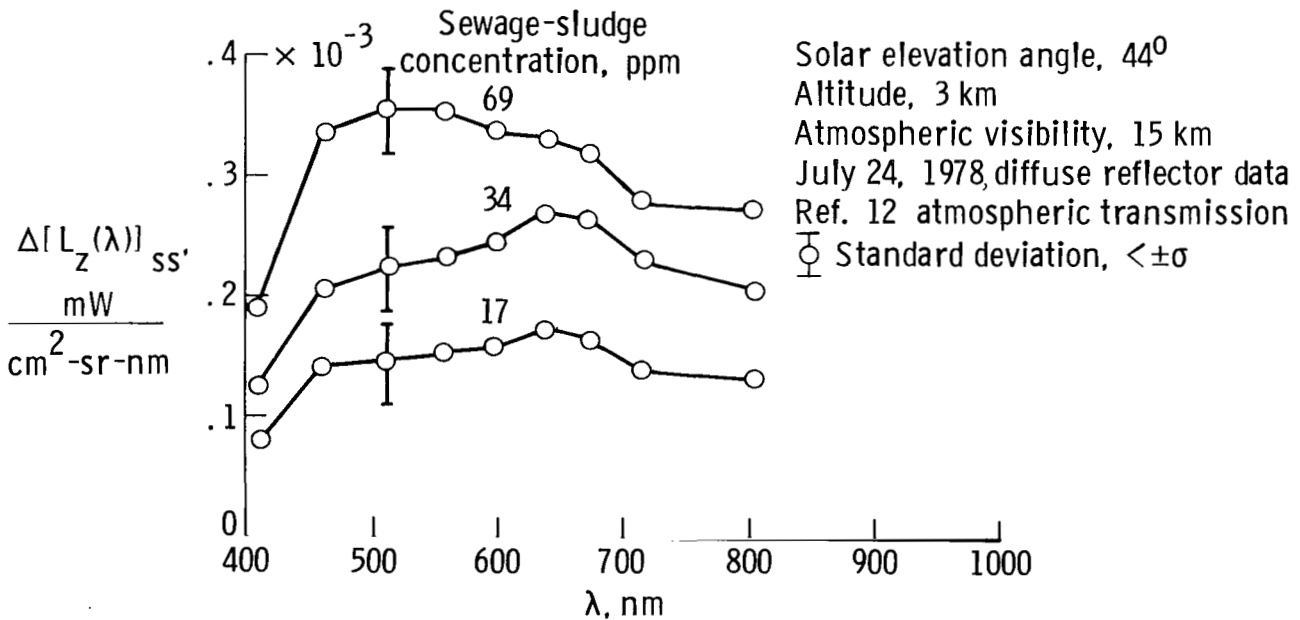(a) Reflectance differences for Back River water laboratory tests.

(b) Calculated radiance differences.

Figure 12.- Comparison of reflectance differences and radiance differences for M^2S instrument and assumed atmospheric conditions.

(a) Aircraft M^2S instrument data.

(b) Calculated values from laboratory results.

Figure 13.- Characteristics of field and extrapolated laboratory results.

1. Report No. NASA TP-1446	2. Government Accession No.	3. Recipient's Catalog No.
4. Title and Subtitle INVESTIGATION OF EFFECTS OF BACKGROUND WATER ON UPWELLED REFLECTANCE SPECTRA AND TECHNIQUES FOR ANALYSIS OF DILUTE PRIMARY-TREATED SEWAGE SLUDGE		5. Report Date August 1979
		6. Performing Organization Code
7. Author(s) Charles H. Whitlock, J. W. Usry, William G. Witte, Franklin H. Farmer, and E. A. Gurganus		8. Performing Organization Report No. L-12694
9. Performing Organization Name and Address NASA Langley Research Center Hampton, VA 23665		10. Work Unit No. 176-30-33-00
		11. Contract or Grant No.
12. Sponsoring Agency Name and Address National Aeronautics and Space Administration Washington, DC 20546		13. Type of Report and Period Covered Technical Paper
		14. Sponsoring Agency Code

15. Supplementary Notes

16. Abstract

In an effort to improve understanding of the effects of variations in background water on reflectance spectra, laboratory tests have been conducted with various concentrations of sewage sludge diluted with several types of background water. The results from these tests indicate that reflectance spectra for sewage-sludge mixtures are dependent upon the reflectance of the background water. Both the ratio of sewage-sludge reflectance to background-water reflectance and the ratio of the difference in reflectance to background-water reflectance show spectral variations for different turbid background waters. The difference in reflectance is the only parameter considered in this study which does not have major spectral variations with different background waters.

17. Key Words (Suggested by Author(s)) Remote sensing Spectral signature Laboratory measurements Environmental monitoring	18. Distribution Statement Unclassified - Unlimited Subject Category 48		
19. Security Classif. (of this report) Unclassified	20. Security Classif. (of this page) Unclassified	21. No. of Pages 33	22. Price* $4.50

National Aeronautics and
Space Administration

Washington, D.C.
20546

THIRD-CLASS BULK RATE

U.S.MAIL

2   1 1U,E,   080679 S00903DS
DEPT OF THE AIR FORCE
AF WEAPONS LABORATORY
ATTN: TECHNICAL LIBRARY (SUL)
KIRTLAND AFB NM 87117

NASA

S

ection 158
Postal Manual) Do Not Return